



Virginia Commonwealth University
VCU Scholars Compass

Theses and Dissertations


Graduate School

2019

ELECTRONIC STRUCTURE OF CATHODE MATERIALS IN LITHIUM ION BATTERIES

John M. Swanlund
Virginia Commonwealth University

Follow this and additional works at: <https://scholarscompass.vcu.edu/etd>

 Part of the [Atomic, Molecular and Optical Physics Commons](#)

© The Author

Downloaded from

<https://scholarscompass.vcu.edu/etd/5851>

This Thesis is brought to you for free and open access by the Graduate School at VCU Scholars Compass. It has been accepted for inclusion in Theses and Dissertations by an authorized administrator of VCU Scholars Compass. For more information, please contact libcompass@vcu.edu.

© John M. Swanlund 2019

All Rights Reserved

ELECTRONIC STRUCTURE OF CATHODE MATERIALS IN LITHIUM ION BATTERIES

A thesis submitted in partial fulfillment of the requirements for the degree of Masters of Science
at Virginia Commonwealth University.

by
John M. Swanlund
M.S. in Physics
Virginia Commonwealth University 2019

Director: Dr. Purusottam Jena, Distinguished Professor, Department of Physics

Virginia Commonwealth University
Richmond, Virginia
May 2019

Acknowledgement

The author wishes to thank several people for their contributions to this work. First and foremost, I offer my most sincere gratitude to Dr. Jena for his leadership, guidance, knowledge, and extraordinary patience. I am indebted to him for his direction and vision. I would also like to thank Swayamprabha Rosy Behera for being my mentor through the early stages of this research and helping lay the framework that was crucial to my work. I also thank Santanab Giri for his early collaboration to identify cathode materials. Thank you to Sam Grey for coaching, organizing, and for being a fountain of positivity when it was most needed. And, finally, to my wife, Kristin, for her love and her support and for being both tranquil and steadfast through the currents of my uncertainty.

Table of Contents

Table of Contents	ii
List of Tables	v
List of Figures.....	vi
Abstract.....	ix
Vita	x
1. Introduction.....	1
1.1 Background	1
1.2 Lithium Ion Batteries	9
1.3 Battery Components.....	11
1.3.1 Cathode Materials	12
1.3.2 Anode Materials.....	13
1.3.3 Electrolytes	13
1.3.4 Solid-Electrolyte Interphase.....	14
1.4 Technical Parameters	16
1.4.1 Energy Density.....	16
1.4.2 Power Density	18
1.4.3 Specific Capacity	19
1.4.4 Self-Discharge.....	20
1.4.5 Cycle Life/Calendar Life	20
1.5 Problems and Risks.....	21
1.5.1 Volumetric Expansion	21

1.5.2	Thermal Runaway	22
1.5.3	Material Scarcity	22
1.5.4	Dendrites	23
1.6	Lithium Ion Battery Summary	24
2.	Theoretical Methods	26
2.1	Born-Oppenheimer Approximation	28
2.2	Hartree Approximation	30
2.3	Hartree-Fock Method	31
2.4	Density Functional Theory	36
2.4.1	Hohenberg-Kohn Formulation	37
2.4.2	Local Density Approximation	39
2.4.3	Generalized Gradient Approximation	41
2.4.4	Hybrid Functionals	42
2.4.5	Basis Sets	43
3.	Methods and Results	46
3.1	Overview	46
3.2	Cluster Materials and Properties	47
3.2.1	Halogens	48
3.2.2	Electron Affinity	49
3.2.3	Vertical Detachment Energy	49
3.2.4	Super Halogens	49
3.2.5	Binding Energy	50
3.3	Results	50

3.3.1	Approach.....	50
3.3.2	Optimized Geometries of Metal Oxides	52
3.3.3	Electron Affinity and Vertical Detachment Energy.....	60
3.3.4	Optimized Geometries of Lithium-Bearing Salts	63
3.3.5	Binding Energy	68
3.3.6	Next Steps	71
4.	Outlook.....	72
4.1	Future of Batteries.....	72
4.1.1	Solid Electrolytes	73
4.1.2	Sodium Ion.....	73
4.1.3	Lithium Air	74
5.	Conclusion	75
	List of References	77

List of Tables

Table 1 Electron affinity and vertical detachment energy of metal oxides currently used in cathodes. Experimental values provided when available	61
Table 2 Electron affinity and vertical detachment energy of metal oxides proposed as candidates for cathode materials. Experimental values provided when available.....	62
Table 4 Calculated binding energies (in eV) of current cathode materials	69
Table 5 Calculated binding energies (in eV) of proposed candidates for cathode materials.	69

List of Figures

Figure 1 Carbon Dioxide Emissions by Sector	4
Figure 2 Energy consumption in the U.S. by fuel type, 2018.....	5
Figure 3 LIB costs are steadily decreasing	7
Figure 4 Schematic of a LIB. Lithium ions are shown intercalated between layers of $LiCoO_2$ in the cathode.	10
Figure 5 Open-circuit energy schematic of a cathode's and anode's chemical interactions with an electrolyte of stability window E_g	15
Figure 6 Comparison of Theoretical Specific Capacities of various cathode materials	19
Figure 7 On the left, an SEI provides a passivating layer; on the right, dendrite growth on the anode short circuits the cell.....	24
Figure 8 Optimized geometries of MnO_2 , FeO_2 , CoO_2 , with neutral on top, anion on bottom. Bond lengths in Å.	53
Figure 9 Optimized geometries of NiO_2 and FeO_4 , with neutral on top, anion on bottom. Bond lengths in Å.	54
Figure 10 Optimized geometries of CoO_4 and NiO_4 , with neutral on top, anion on bottom. Bond lengths in Å.	55

Figure 11 Optimized geometries of <i>MoO4</i> , with neutral on top, anion on bottom. Bond lengths in Å.....	56
Figure 12 Optimized geometries of <i>Mn2O4</i> , with neutral on top, anion on bottom. Bond lengths in Å.....	57
Figure 13 Optimized geometries of <i>AlO2</i> and <i>VO3</i> , with neutral on top, anion on bottom. Bond lengths in Å.	58
Figure 14 Optimized geometries of <i>CoO3</i> and <i>FeO5</i> , with neutral on top, anion on bottom. Bond lengths in Å.	59
Figure 15 Optimized geometry of <i>CrO4</i> , with neutral on top, anion on bottom. Bond lengths in Å.....	60
Figure 16 Electron affinities of investigated metal oxides	63
Figure 17 Optimized geometries of <i>LiMnO2</i> and <i>LiFeO2</i> . Bond lengths in Å.....	64
Figure 18 Optimized geometries of <i>LiCoO2</i> and <i>LiNiO2</i> . Bond lengths in Å.	65
Figure 19 Optimized geometries of <i>LiFeO4</i> and <i>LiCoO4</i> . Bond lengths in Å.....	65
Figure 20 Optimized geometries of <i>LiNiO4</i> and <i>LiMoO4</i> . Bond lengths in Å.	65
Figure 21 Optimized geometries of <i>Li2MoO4</i> and <i>LiMn2O4</i> . Bond lengths in Å.	66
Figure 22 Optimized geometry of <i>Li2Mn2O4</i> . Bond lengths in Å.	66

Figure 23 Optimized geometries of <i>LiAlO2</i> and <i>LiVO3</i> . Bond lengths in Å.	67
Figure 24 Optimized geometries of <i>LiCoO3</i> and <i>LiFeO5</i> . Bond lengths in Å.	67
Figure 25 Optimized geometry of <i>LiCrO4</i> . Bond lengths in Å.	68
Figure 26 Binding Energy of current and proposed cathode materials.....	70

Abstract

ELECTRONIC STRUCTURE OF CATHODE MATERIALS IN LITHIUM ION BATTERIES

By John M. Swanlund, M.S.

A thesis submitted in partial fulfillment of the requirements for the degree of Master of Science at Virginia Commonwealth University.

Virginia Commonwealth University, 2019

Major Director: Dr. Purusottam Jena, Distinguished Professor, Department of Physics

Lithium ion batteries are ubiquitous in modern life, from powering hand-held electronic devices to electric vehicles. And with the necessary drive toward renewable energy sources like solar and wind, electricity storage for the grid promises to drive up the demand for higher performing, less expensive, safer, and more environmentally friendly secondary batteries. Recent research has theorized that replacing halogens in batteries' electrolytes with non-halogens can yield desirable performance characteristics while eliminating the most dangerous and problematic chemicals. This thesis explores the possibility that a similar approach can be taken with the cathodes of lithium ion batteries. The active material in a cathode is a salt composed of an alkali cation – the positive lithium ion, and a negative ion – usually a metal oxide. Replacing the negative ion with a superhalogen, which is more electronegative than the most electronegative element, may yield comparable electronic properties to current cathode materials while also opening up opportunities to research materials previously not considered for lithium ion battery cathodes.

Vita

John Martin Swanlund was born on September 21, 1970, in Jacksonville Florida, and he is an American citizen. He graduated from Green Run High School in Virginia Beach in 1988. He received his Bachelor of Science in Physics and Computer Science from University of Mary Washington, Fredericksburg, Virginia in 1993.

1. Introduction

1.1 Background

The ability to store energy has always been a key to human comfort and convenience. Burning wood and coal allows us to carry the potential of light and heat from the outdoors into our homes. We are not beholden to the energy delivered instantaneously by the sun, which is easily blocked by our shelter, by clouds, or by the Earth as it rotates us into shadow each night. We can carry our fuel onto a ship and power engines instead of being slave to the winds. For millennia, we harnessed the fuels found in the forests and underground. Into the 20th century, our lives were transformed by conversion of chemical energy to mechanical energy and heat. With wood, coal, petroleum, and other available sources, we were lighting and heating our homes, cooking our food, and driving our cars.

But then a separate revolution occurred. Public spaces and homes were wired for electricity, and suddenly, lighting and heating had an apparent clean and safe source. An extraordinary level of convenience was achieved. Lighting our rooms no longer required a local flame; the flip of a switch provided instant light. We brought motors indoors for mundane tasks like washing our clothes and for less mundane tasks, like the decadent luxury of air conditioning.

Next came the drive for an untethered source of electricity – batteries. For instance, lead acid batteries were coupled with a starter motor to automate the initial cranking of internal combustion engines. These batteries were also readily recharged with an alternator driven by that

same engine the battery helped start. Alkaline batteries provided ultimate hand-held portability to power devices like flashlights. And since we could now carry a source of electricity in our pockets, a revolution in portable electronics soon followed with devices like the transistor radio.

We were no longer tethered to an electrical outlet or burdened by household-appliance-sized electronics. But we were hindered by the limits of disposable, single-use batteries. Constantly buying alkaline batteries is expensive, and disposing of their constituent heavy metals and toxic chemicals is a burden to the environment. A quiet race began. Soon, advancements in electronics miniaturization would make disposable batteries the weakest link in electronic devices.

Rechargeable batteries would emerge first as a convenience (avoiding trips to the store to buy more single use batteries and avoiding special disposal requirements) but quickly became necessities. The current pinnacle of portable electronics is the smart phone – an amazingly capable computer, camera, and communications device that fits in our pockets. This device requires an equally portable and capable power source.

The revolutionary value of batteries comes from their portability, but even when portability is not a goal, batteries can provide flexibility to serve multiple applications. They are integral in home smoke detectors, and provide convenience for things like wall-mounted clocks. Batteries allow these devices to be installed in places where an AC power outlet is not nearby. In addition, batteries are the foundation for an uninterruptable power supply (UPS). For a UPS, and often for smoke detectors and alarm clocks, batteries provide continuous power when the wired AC electricity fails. Requirements for these static applications vary. A clock generally needs low

voltage delivered over a long duration. A smoke detector demands a reliable back-up power source that lasts its prescribed lifetime. A UPS must deliver higher voltage to mimic the AC wired system, but it must reliably manage being constantly depleted over time then recharged.

From convenience to mission-critical applications, batteries have become ingrained in our lives. But we are now at the precipice of another leap in the application of energy storage. Robust energy storage is becoming more than a matter of convenience; it is an imperative. Beginning in the Industrial Age, the burning of fossil fuels has increased carbon dioxide and other greenhouse gasses in the atmosphere. This has led to warming of the Earth's oceans and melting of land ice. As our dependence on fossil fuels has increased over the decades, and with huge emerging economies in China and India, the rate we are pumping carbon dioxide into the atmosphere is increasing. Melting ice and warming oceans are leading to sea level rises that are already catastrophic in low-elevation areas like Miami, Florida and New Orleans, Louisiana. Sea levels have risen by about 7 cm since 1993¹, and they are projected to rise between 9 and 18 cm over 2000 levels by 2030. This has resulted in high tide, "sunny day" flooding in cities like Miami, where hundreds of millions of dollars are being spent on anti-flooding infrastructure².

Furthermore, flooding becomes an even greater concern when storms emerge. A strong Atlantic hurricane can bring a devastating storm surge to a coastal city. When that city is already under the strain of "sunny day" flooding, hurricanes will be even more catastrophic. Adding to this tropical storm powder keg, increasing ocean heat is leading to more frequent and more powerful storms than ever before. Recently, the United States was ravaged by several powerful tropical

storms, many of which are historically devastating. In 2017, Hurricane Harvey dumped a record amount of rain, over 1500 millimeters of rain. In 2018, Hurricane Michael hit landfall in Florida as the third most intense cyclonic storm on record, only weeks after Hurricane Florence dropped over 900 millimeters of rain on the Carolinas.

In order to arrest the increasing warming of our planet, it is imperative that we dramatically reduce our dependence on fossil fuels. Transportation accounts for about 28% of greenhouse gas emissions in the United States³, so cleaner improvements in this sector would have significant positive impact on future emissions.

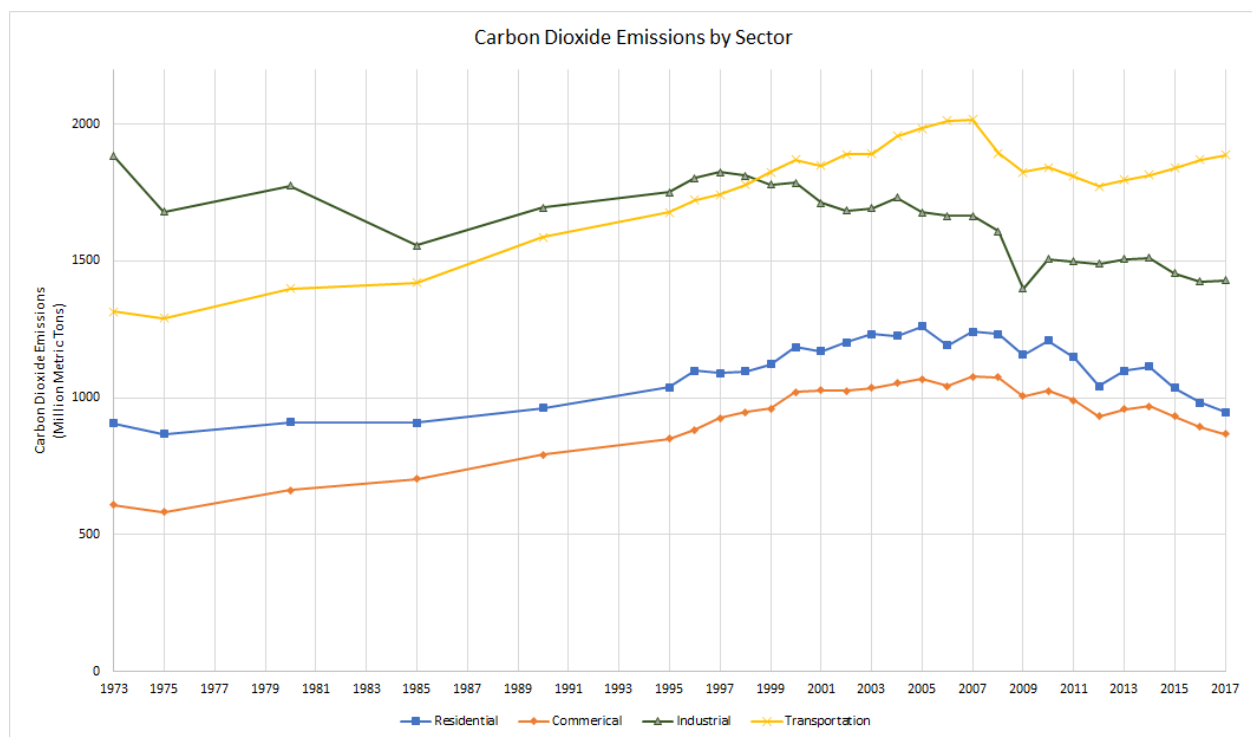


Figure 1 Carbon Dioxide Emissions by Sector⁴

Electric Vehicles (EVs) offer some promise to help alleviate this burden by shifting from burning petroleum in internal combustion engines to storing and delivering power generated from clean renewable sources. Transitioning 30% of internal combustion engines for transportation to EVs would result in a 22% reduction in petroleum demand.⁵ In addition, renewable energy sources must become more prevalent. In 2017, about 80% of the energy consumed in the United States came from fossil fuels, and about 11% was from renewable sources.⁶

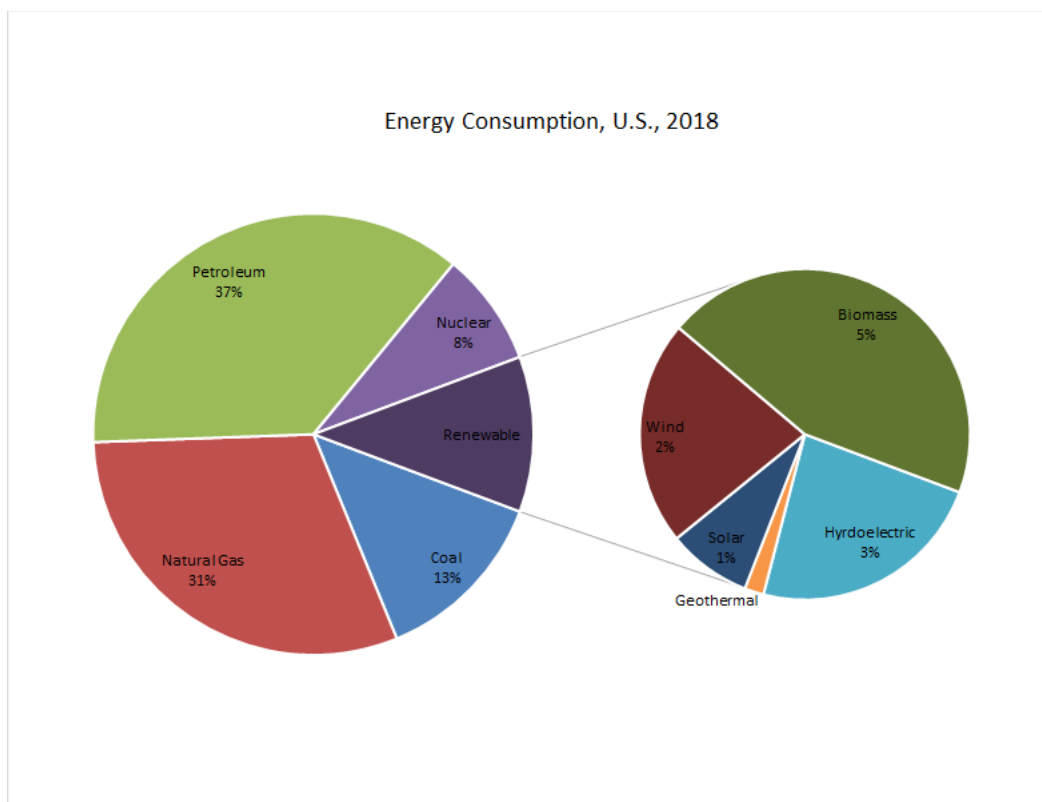


Figure 2 Energy consumption in the U.S. by fuel type, 2018⁴

Increasing the ratio of renewable energy will certainly require public commitment, but it will also depend on overcoming technical and economic challenges.

Currently, hydroelectric sources provide the most prevalent renewable energy in the United States. Solar and wind power generation are increasing. However, the availability of the sun as a source for solar power generation is guaranteed to be intermittent. Depending on the geographical location, wind sources might be more reliable, but they are still slave to the whims of the weather. These fluctuating sources need to be augmented with an energy storage strategy. A solar array may produce more energy during peak daylight than demand requires, so the surplus energy can be stored in huge secondary battery systems and delivered to electricity consumers when the sun goes down. A similar strategy can be employed for non-renewable electricity generation. A coal burning plant might produce surplus energy during off-peak hours (for instance, during the cooler nighttime hours of the summer) and store that surplus in a battery. This surplus can then be provided to customers during times of peak demand. Additionally, power generation could be co-opted to smaller producers across the region, stored centrally by the primary provider, and then delivered as required by consumer demand. Batteries are a perfect fit for such applications, and lithium ion technology is currently the front runner among the choices of rechargeable batteries.

Lithium ion batteries (LIBs) are well suited to a variety of applications, including portable electronics like smart phones, electric vehicles (EVs), and electronic grid energy storage. As will be discussed in more detail later in this thesis, LIBs have several properties that make them widely popular across functions. They have higher cell potential than other rechargeable batteries. LIBs also have higher energy density and higher capacity than other battery

chemistries, so portable electronics can be smaller and lighter than with alternatives.⁷ Cost of LIBs has been a factor over the last couple decades, but with research and materials advancements, costs are declining.

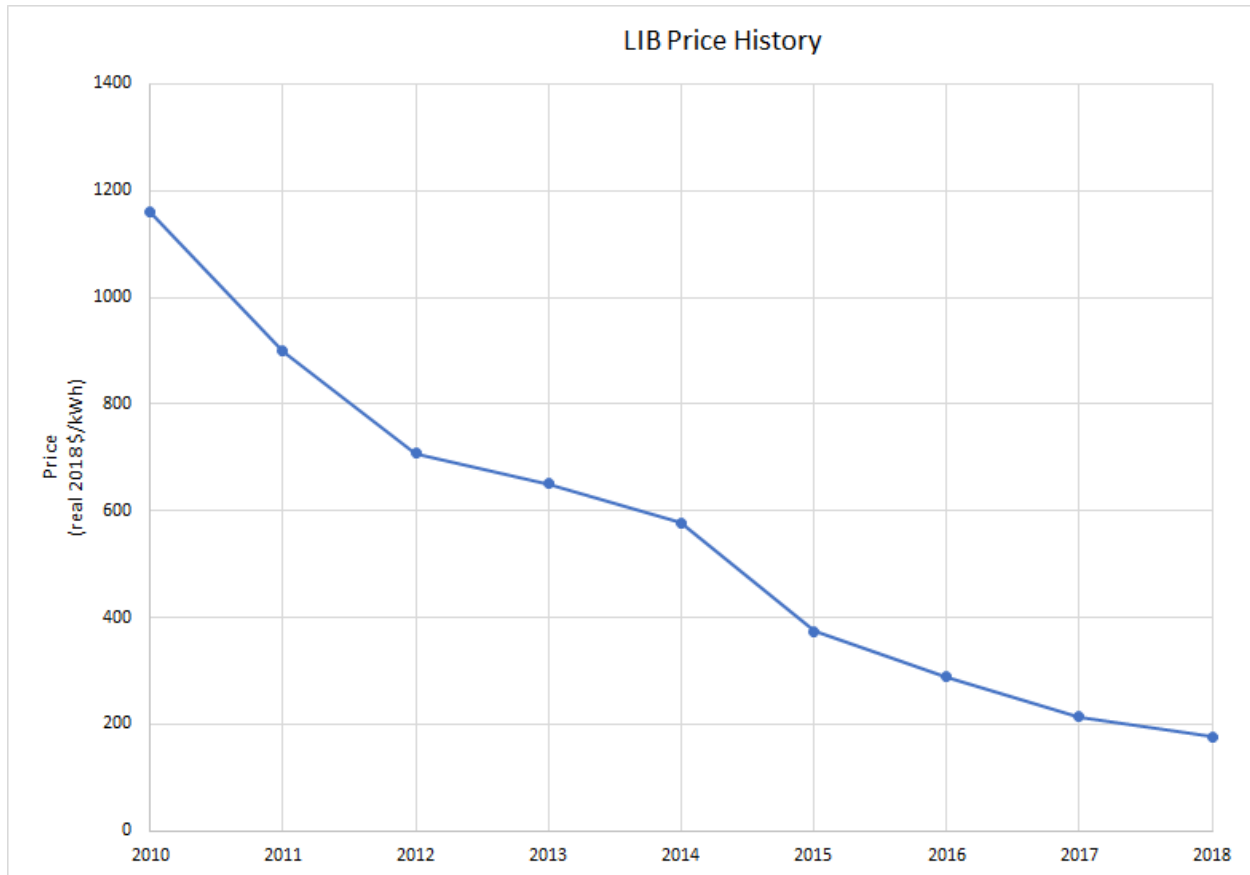


Figure 3 LIB costs are steadily decreasing⁸

In addition to the electronic properties, there are other considerations for the success of an energy storage technology. Safety is always a paramount concern. For many of the same reasons that make them desirable, LIBs can become dangerous if mishandled or damaged. Fully charged, they can store a surprising amount of energy for their size and weight. Being portable and

ubiquitous, smart phones with their potent LIBs often fall victim to human clumsiness and neglect. This can lead to rapid and catastrophic discharge, and, potentially, brief YouTube fame.

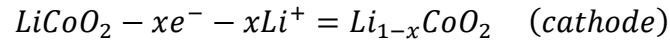
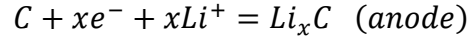
Furthermore, the safety and availability of materials is a factor for a battery technology's long-term sustainability and cost-effectiveness. Lithium, itself, is not especially rare on Earth; however, mining reserves are generally localized in South America, Australia, and Asia. Cobalt, which has been a primary fixture in LIB cathodes, is not especially abundant and is also toxic and expensive to handle. A goal of this research, discussed in more detail below, is to investigate alternative cathode materials with similar electronic properties that are safer and make use of abundant elements.

Both the convenience and necessity of energy storage have made lithium ion batteries a common component in everyday life. We demand a low profile and long life from our smart phone batteries, and car manufacturers are all working diligently to engineer EVs with ranges comparable to internal combustion engines. Moreover, as the world transitions to greater reliance on renewable energy sources, rechargeable batteries will have increased importance in preventing power disruptions. Energy grid storage, electric vehicles, and portable electronics all demand capabilities that LIBs can deliver. With research and development into new battery chemistries, to which this thesis hopes to contribute perhaps a tiny drop, progressing at a fever pitch, LIBs will be tightly coupled with our future technological achievements.

1.2 Lithium Ion Batteries

A battery is a familiar and versatile means of storing portable energy. It is made up of electrochemical cells, which deliver electrical energy through chemical reactions internal to the cell. Electrochemical cells have three basic parts: the negative electrode (anode), the positive electrode (cathode), and the electrolyte, separating the two electrodes. In lithium ion batteries, the cathode is usually a transition metal oxide, like $LiCoO_2$. The anode is usually porous graphite, and the electrolyte is a lithium salt in an organic solvent. In LIBs (and other battery types, like lead-acid batteries), there is also a permeable membrane separating the anode and cathode. This membrane allows charge carriers to pass through but prevents short circuiting between electrodes.

In a charged battery, the anode stores the working Li^+ ions, along with delocalized electrons to balance the ions and make the anode electrically neutral. To make use of the battery, an electrical circuit is closed between the anode and the cathode. The anode undergoes an oxidation reaction, and the electrons resulting from that reaction flow into the circuit from the lower electrical potential of the anode toward the higher electrical potential of the cathode. Simultaneously, the positive lithium ions resulting from the oxidation reaction are conducted within the cell through the electrolyte from the anode, with high lithium chemical potential, toward the cathode, which has lower lithium chemical potential.⁹ In the cathode, the lithium ions are inserted into the cathode material through a process called intercalation¹⁰.



The electrolyte and separator membrane allow ionic transport but prevent spontaneous electrical discharge.

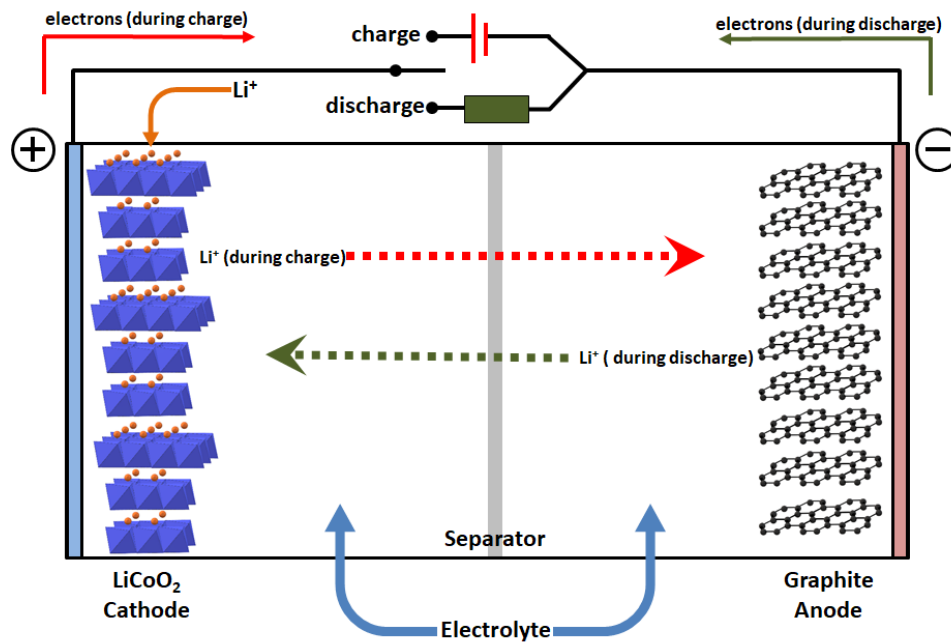


Figure 4 Schematic of a LIB. Lithium ions are shown intercalated between layers of $LiCoO_2$ in the cathode.

The battery is considered fully discharged when the voltage in the circuit between the anode and the cathode drops below some threshold making the battery unsuitable for its intended purpose.

When being charged, an external electrical potential places the anode at a higher electrical potential than the cathode, causing electrons and ions to go in the opposite direction than

described above. Positive lithium ions flow from the cathode, through the electrolyte, and amass in the anode with the surplus electrons from the circuit.

Note that during the recharge cycle, to be completely accurate, some of the labels on the battery diagrams should be swapped. The component that is the anode of a fully charged battery becomes the cathode during charging, and the cathode of a fully charged battery becomes the anode. Technically, lithium ions always flow from the anode (the negative electrode) to the cathode (the positive electrode). For the sake of brevity, clarity, and consistency with industry literature, in this thesis the electrodes are referred to by their roles during discharge. In **Figure 4** above, the electrode on the left is labeled the cathode, although, technically, it is the anode during recharging. Similarly, the electrode on the right is labeled the anode, though it is serving the role of the cathode during recharge.

1.3 Battery Components

There are several factors that come into play when assessing the performance of a battery. These factors include energy density, power density, capacity, rate capability, self-discharge, cycle life, and calendar life. Each of these factors is discussed in more detail below. The suitability for a type of battery in an application may depend on many or all of these factors in addition to size constraints, portability, safety, and cost.

1.3.1 Cathode Materials

As mentioned above, cathodes of LIBs are usually metal oxides. These metal oxides are covalently bonded to form stable compounds and are arranged with crystal structures in which lithium ions can be stored or released reversibly.¹¹ The cathode materials must be multivalent in order to find electrical neutrality in both the presence and absence of the mobile lithium ions.

Common materials used in modern LIBs are lithium cobalt oxide (LCO) – $LiCoO_2$, lithium manganese oxide (LMO) – $LiMnO_2$, lithium iron phosphate (LFP) – $LiFePO_4$, lithium nickel manganese cobalt (NMC) – $LiNi_xMn_yCo_zO_2$, and lithium nickel cobalt aluminum oxide (NCA) – $LiNiCoAlO_2$. Cathode materials are chosen for specific applications based on various technical parameters described below. Some provide higher specific energy than others, while some offer higher specific power density. Safety and lifespan are also considerations. For instance, LCO has a high specific energy but a comparatively low power density, so it is suitable for a wide range of uses, including portable electronic devices. However, of the common cathode materials, LCO is among the lowest in thermal stability¹², so it is not suitable for high temperature applications. Manganese is less toxic and less expensive than cobalt and nickel, so LMO is an appealing material for cathodes.⁷ However, manganese-based cathodes have problems with their internal structural stability, leading to decreased capacity and increased impedance.⁷ Many performance enhancements in recent years have come from formulating a combination of cobalt, nickel, manganese, and other elements to achieve a desirable balance of properties.

1.3.2 Anode Materials

The most common, and nearly ubiquitous, anode material in modern LIBs is graphite. Each lithium ion intercalates within an arrangement of six carbon atoms to form LiC_6 .¹³ Proposed in 1977, graphite is an ideal material in many respects – it is stable, non-toxic, bountiful, and inexpensive.¹⁴ It has led to vastly safer batteries than its predecessor, lithium metal. Lithium metal has several performance advantages – for instance, higher energy density, power density, and open circuit voltage – but is more expensive, more toxic, and prone to dendrite formation and, thus, catastrophic short circuiting.

1.3.3 Electrolytes

Electrolytes provide the medium through which lithium ions flow from anode to cathode. They must be good conductors of lithium ions, but they also must discourage the flow of electrons through the battery. Electrolytes are a combination of salts and solvents. The salts are often a combination of multiple lithium salts, common examples being $LiAsF_6$, $LiBF_4$, $LiFePO_4$, $LiClO_4$, $LiN(SO_2F)_2$, and $LiN(SO_2CF_3)_2$. Usually, organic solvents, like dimethyl carbonate and ethylene carbonate are combined with the lithium salts to complete the electrolyte.

Electrolytes bridge the difference in redox energies between the cathode and anode. The electrolyte's HOMO and LUMO must be in the ranges of the redox energies of the cathode and anode, respectively.¹⁵ An ill-suited electrolyte will either reduce the open circuit voltage of the

battery, cutting into the overall performance capabilities of the battery, or result in an unstable battery.

1.3.4 Solid-Electrolyte Interphase

The interfaces between electrodes and electrolyte are also important in the function and life of a battery. A battery's cycle life depends primarily upon the interfaces at both the anode and cathode.¹⁶ Unintended reactions at the electrode-electrolyte interface are the primary reason for reduction in the lifetime of a battery. However, these reactions have also become part of the engineering of cells. Upon the battery's first charge, a chemical reaction can take place between the electrode and electrolyte, forming a solid-electrolyte interphase (SEI) layer. The SEI must allow lithium ions to pass through easily and can actually improve the chemical stability of the battery by providing a passivating surface layer between electrode and electrolyte.

The SEI establishes a passivation layer between the electrodes and electrolyte and improves the stability of the components by expanding the stability window of the electrolyte.¹⁵ For instance, if the highest unoccupied molecular orbital (HOMO) of the electrolyte is above the electrochemical potential of the cathode, μ_c , the electrolyte will be oxidized by the cathode. However, the SEI can provide a buffer to block those highest occupied molecular orbitals from reacting with the cathode. Similarly, an SEI might block reduction of the electrolyte by the anode even if the electrochemical potential of the anode, μ_a , is above the electrolyte's LUMO.¹⁷ This

passivating layer allows a greater open-circuit voltage (V_{oc}) than from the electrodes without an SEI.

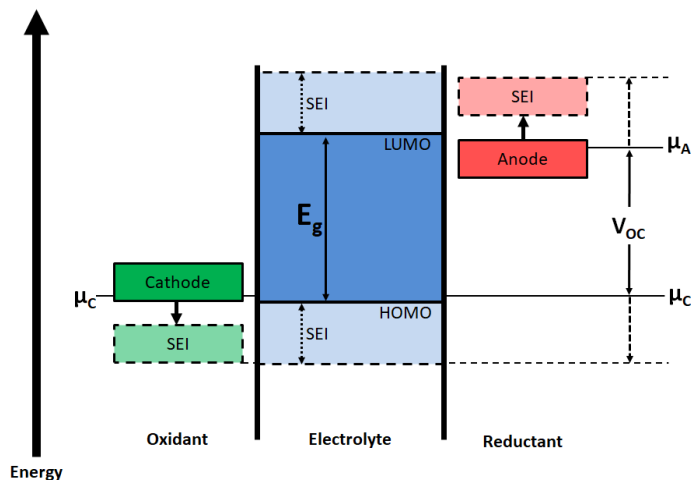


Figure 5 Open-circuit energy schematic of a cathode's and anode's chemical interactions with an electrolyte of stability window E_g .^{15, 17}

SEI necessarily reduces the capacity of the battery by permanently locking up active material that could otherwise be serving the battery's commercial purpose. While there has been research into the electrode-electrolyte interface, this is an area where there is still much room for advancement. The processes behind the formation of the SEI is complex and neither well-understood nor robustly researched.¹⁸

1.4 Technical Parameters

1.4.1 Energy Density

Energy density is the amount of energy that can be stored by a battery in relation to either the volume or mass of the battery. When comparing batteries, a higher energy density means that the battery will deliver a charge over a longer time, everything else being equal.

Without additional qualification, the term “energy density” usually refers to volumetric energy density. Engineering a battery with high volumetric energy density leads to a device with lower volume. Volumetric energy is typically expressed in units of Watt-hours per liter ($\text{W}\cdot\text{h}\cdot\text{L}^{-1}$). A lithium ion has one of the smallest radii of any charged particles, so LIBs have an advantage over other technologies in achieving high volumetric energy density.⁷ High volumetric energy density allows for long-lasting portable electronic devices for which size is a premium, like smart phones and laptop computers. It also allows more cells to be packed into a confined footprint, like in an EV, ultimately contributing to increasing the vehicle’s range. Stationary installations, like grid storage, place a low premium on gravimetric or volumetric considerations.

Gravimetric energy density, also referred to as specific energy, is the energy that can be stored in a battery relative to the battery’s mass. It is usually represented in units of Watt-hours per kilogram ($\text{W}\cdot\text{h}\cdot\text{kg}^{-1}$). As with volumetric energy density, lithium’s place on the periodic chart gives it an advantage with gravimetric energy density. Lithium is the third lightest element and the lightest of metals, so a battery based on lithium has a head start over other chemistries.⁷

Also, as with volumetric energy density, gravimetric energy density is an important consideration for portable electronic devices, since the weight of the device is a significant facet in its portability and its overall aesthetic. For instance, the Google Pixel 2 smartphone is listed as having a mass of 142 grams.¹⁹ The battery is 100 grams, more than 2/3rds the overall mass of the product.²⁰ In addition, gravimetric energy density is certainly a consideration with EVs, since the vehicle's mass affects its range. A lighter battery pack (with other parameters being equal) will lead to a more efficient vehicle and, thus, greater range. Energy density of LIBs has increased about $5 \text{ W}\cdot\text{h}\cdot\text{kg}^{-1}$ every year since their inception in the early 1990s, and it is now over $160 \text{ W}\cdot\text{h}\cdot\text{kg}^{-1}$.²¹

Comparing gravimetric and volumetric energy densities of LIBs to other battery technologies highlights the advantages of LIBs. For instance, while lead-acid batteries have been used for automotive starters for over a century, their volume and weight have not been a critical factor in their success. The battery is mounted to the frame and the car hauls it around without complaint. Lead acid batteries are cost effective, but they have a low energy density of 30 to $40 \text{ W}\cdot\text{h}\cdot\text{kg}^{-1}$.²² Our ubiquitous hand-held electronics require light weight, small spatial footprint, and on-demand electricity to meet performance demands, and lead-acid batteries fall short of meeting those requirements. Nickel-cadmium (Ni-Cd) batteries peaked in popularity in the 1990s but were quickly supplanted by LIBs, which boast energy densities up to three times that of Ni-Cd batteries.¹⁶ A key to the success of LIBs in our day-to-day lives is their greater energy storage by both weight and volume, as measured by their energy densities.

1.4.2 Power Density

Power density refers to the amount of power that can be delivered by a battery in relation to either mass or volume. It is a measure of the time necessary to charge or discharge the battery.²³

When comparing batteries, higher power densities are suited for more power-demanding applications like electric vehicles and power tools. Handheld electronics can easily sacrifice power density for improved energy density.

Usually, the term power density refers to gravimetric power density, or specific power. It is power per unit mass, so it is often reported in units of Watts per kilogram ($\text{W}\cdot\text{kg}^{-1}$). However, other factors than mass affect performance, like microstructure of the electrode materials. And while the electrodes host the active material, inactive components can add to a battery's mass and volume, diluting power density as an effective comparative measure.

Charge and discharge rate is another power metric, and it may be more useful as a measure of a battery's actual performance.²³ A rechargeable battery's rate capability, or C-rating, is a comparative measure of the current that the battery can deliver over an hour. Stated another way, it is the inverse of the amount of time required to completely charge or discharge a battery at a certain current. For instance, if a battery's capacity has been rated $2,400\text{ mA}\cdot\text{h}$, discharging the battery at 1.0 C means applying a load of 2,400 mA for an hour. Discharging the battery at 0.5 C means applying a load at 1,200 mA, where the battery will fully discharge in two hours. The

same comparative measure applies to charging. Charging a 2,400 mA·h battery at 4,800 mA is 2.0 C.

1.4.3 Specific Capacity

Specific capacity is a measure of how much current can be drawn from a battery over time per unit volume. It is often reported in units of milliamperes-hours per gram ($\text{mA}\cdot\text{h}\cdot\text{g}^{-1}$).

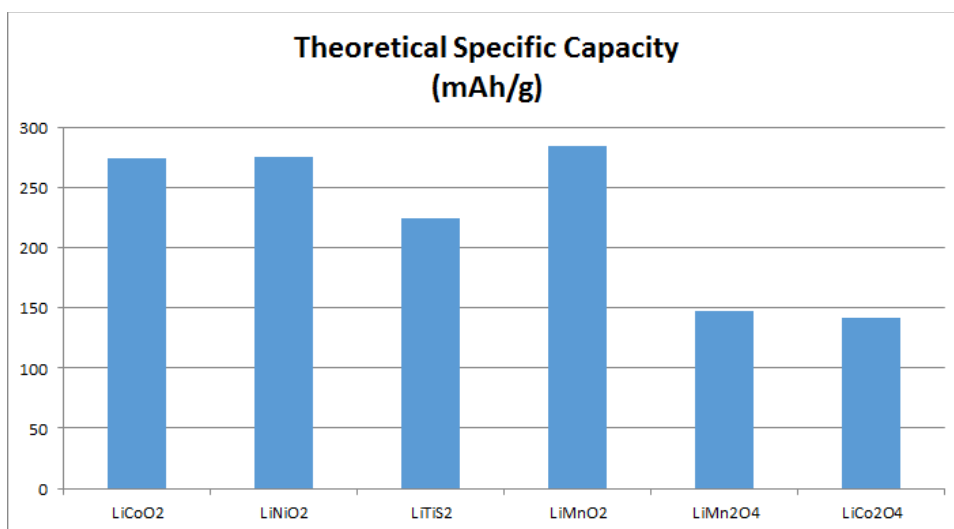


Figure 6 Comparison of Theoretical Specific Capacities of various cathode materials

When a consumer electronic device like a cellphone is powered by a rechargeable battery, the sales literature will often cite the battery's capacity as a selling point. In this circumstance, capacity is usually reported in milliamperes-hours, without the volume factor. From a consumer's perspective, this allows devices to be compared in terms of their overall utility to the consumer since this measure of capacity can factor in, among many other things, the size of the battery.

Simply stated, with everything else being equal, a larger battery (that is, a battery with higher mass of electrochemically active materials) will provide a longer charge than a smaller battery.

Capacity is also dependent upon the composition of electrodes, particularly the cathode. When a battery is constructed, the cathode provides all of the working lithium ions that will serve the battery's purpose. The lithium content that can be reversibly intercalated within the cathode determines the capacity of the battery.²⁴ The anode is sized to accommodate these ions.

1.4.4 Self-Discharge

All batteries discharge when left idle for some duration of time. Anyone who has tried to start a car that has been unused for a couple months knows that lead-acid batteries lose their effectiveness when not charged. Alkaline batteries installed in smoke detectors certainly don't last indefinitely, usually leading to late night chirping. Contemporary LIBs have a relatively low self-discharge rate of less than 10% per month, compared to other rechargeable technologies, like 20% for Ni-Cd batteries and 30% for NiMH batteries.²⁵

1.4.5 Cycle Life/Calendar Life

Over its lifetime, a battery may be recharged hundreds, or, perhaps, even thousands, of times. Each recharge can result in miniscule structural changes in the electrode materials or irreversible chemical reactions between the electrolyte and electrodes.

1.5 Problems and Risks

1.5.1 Volumetric Expansion

In a LIB, lithium ions are intercalated within both the anode (during charging) and the cathode (during discharge). This is not a chemical reaction in which molecules are transformed, but, instead, the lithium is inserted into the layers of electrode material. In the case of the anode, lithium is embedded within layers of graphite; in the cathode, layers of metal oxide receive the lithium ions. Both of these processes are reversible, leading to the extraordinary ability of LIBs to be charged and discharged so effectively. However, insertion of lithium in the electrode materials necessarily results in some degree of increase in volume. Likewise, de-insertion leads to volume decrease. Considering the demands placed on their size, batteries have to be carefully designed to allow for expansion and contraction. In addition, any rigid structure within the battery, whether part of the battery's engineering or a result of a side reaction between chemicals in the electrodes and electrolyte, might not flex adequately to survive the periodic swelling and compression of during battery use. Particularly susceptible are the protective SEIs that form on the surface of the electrodes. Over time, these repeated expansions and contractions can result in continued deposition of SEI materials and consumption of electrolytes, leading to decreased capacity, limited battery performance, and even battery failure through short circuiting.²⁶ Some materials are less susceptible to volume changes than others, so this must be another facet in the engineering of the battery in order to keep safety paramount while also meeting design requirements.

1.5.2 Thermal Runaway

Battery technologies are engineered to balance various performance characteristics with safety. Each battery design has a normal operating temperature range, and at some point above that range, the materials in the battery become thermally unstable. Unintended defects in manufacturing can lead to decreased performance of the battery, but if the defects are severe enough, they can lead to a short circuit in a battery cell, causing an increase in temperature. If the cell temperature reaches catastrophic levels, it could increase temperatures throughout the battery, including adjacent cells, amplifying the catastrophe. Incidents like the 2006 Sony laptop battery recall and dramatic Hoverboard fires in 2015 had manufacturing defects and thermal runaway at their roots.²⁷

1.5.3 Material Scarcity

While, to some degree, every element available to us on Earth is limited, many are so abundant that we should have no concern about them becoming scarce. Lithium is, clearly, at the heart of a lithium ion battery, and it is generously abundant on Earth. Unfortunately, the near-limitless supply is locked in sea water and is costly to extract.²⁸ Our current supplies come from concentrated brines located in Bolivia, Chile, and a few other countries, with a host of environmental and humanitarian issues arising from commercial lithium mining. Nitrogen and oxygen are abundant in our atmosphere; hydrogen and oxygen are abundant in our oceans; oxygen and silicon are abundant in Earth's crust. Aluminum makes up about 8.2% of the crust,

and iron makes up 5.6%. Both are relatively abundant and inexpensive to source. However, in the case of cobalt, for instance, only 0.0029% of Earth's crust is composed of this transition metal. It may not be considered scarce at the moment, but the relative low abundance raises a couple concerns. First, it is more expensive to source than more abundant materials. It may require processing of more raw material to get a smaller amount, thus making it more expensive and more environmentally impactful to source. It might be practical to source it from only a few locations globally, leading to transportation and other logistical considerations. And, finally, when the ready sources of the material are consumed, it will truly become scarce, increasing its cost as well as the human and environmental impact to find and exploit new sources. At some point, it may become cost-prohibitive to the point of being unavailable. In the constant tug of supply-demand-cost, research must pursue new materials to replace those whose scarcity move them beyond reach of their intended application. These new materials, ideally, will be abundant for the foreseeable future and inexpensive to source.

1.5.4 Dendrites

Dendrites are branch-like formations of lithium atoms that can develop on the electrodes, particularly the anode, over the course of charging and discharging. At their most benign, they can lead to decreased cycling efficiency and capacity loss. However, they are especially dangerous in LIBs because they can lead to a short circuit between the electrodes, causing catastrophic electrical discharge. Batteries with a liquid electrolyte are more susceptible to dendrites than batteries with solid electrolytes. In addition, charging a battery at a high voltage

can expedite dendrite growth; this becomes an engineering challenge as consumers demand faster charging. As worrisome as dendrites are for LIBs, they are even more problematic in lithium metal batteries.²⁹ Dendrites constitute one of the biggest hurdles of implementing a pure lithium anode.

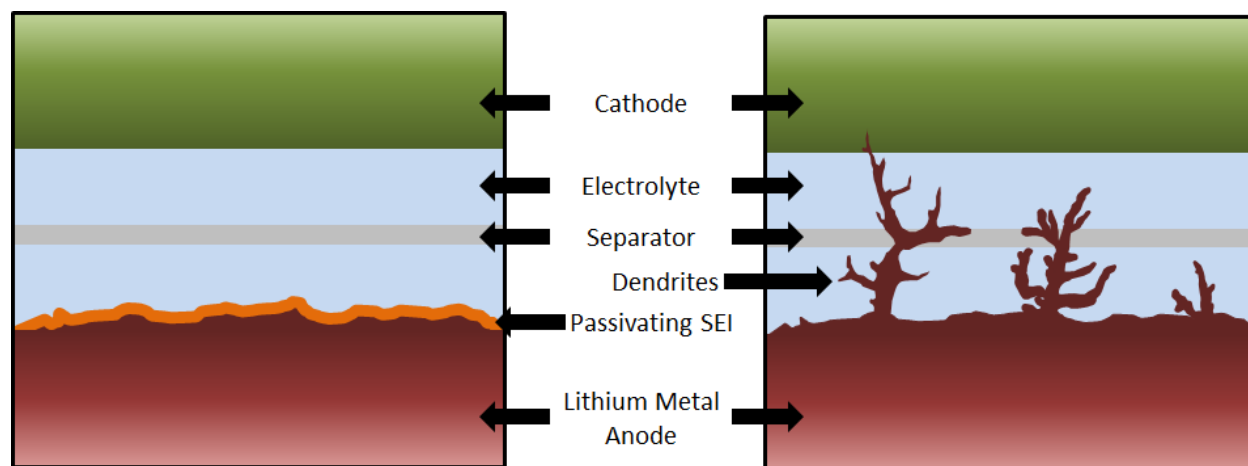


Figure 7 On the left, an SEI provides a passivating layer; on the right, dendrite growth on the anode short circuits the cell

The formation of a solid-electrolyte interface (SEI), as discussed above, can guard against formation of dendrites. In addition, a polymeric membrane is included in the battery to separate the electrodes to prevent dendritic growth. Such a membrane allows the conduction of ions but blocks the flow of electrolyte solution, thus helping prevent dendrites.³⁰

1.6 Lithium Ion Battery Summary

While the science continues to advance the understanding of LIBs and their components, there is still room to learn and improve. Improving the design of the next generation of batteries is not an

easy task because it involves current limitations on anodes, cathodes, and electrolytes, as well as the interfacial problems between electrode and electrolyte. Much of the current research is addressing the shortcomings in these components. For instance, graphite anodes in commercial LIBs are hindered by low specific capacity and low rate capacity, limiting their future utility in booming fields of consumer electronics and EVs.³¹ Implementing higher capacity anode materials, like lithium metal, is currently not feasible because the end products are unstable and dangerous.

Cathodes can be a problem area in batteries out of concerns for cost and safety of their materials, like cobalt. In addition, thermal runaway within the cathode must be a consideration when designing a battery. Side reactions can liberate oxygen which can lead to increased heat generation and thermal instability.

Electrolytes can leak; they can be toxic, flammable, explosive, corrosive, and can limit a battery's lifespan in several ways.³²

Work is currently underway to improve these deficiencies because the steady march of incremental (and sometimes revolutionary) advancements will quickly find their way to the competitive and demanding marketplace of energy storage. This thesis focuses on the design of cathode materials, with the hopes of understanding the current state of the art and, perhaps, contributing some thoughts to the direction of some future experimental investigations.

2. Theoretical Methods

Our theoretical method starts with solving the time-independent non-relativistic Schrödinger equation:

$$\hat{H}\Psi = E\Psi \quad (2.1)$$

Here, Ψ is the system's wave function, and \hat{H} is the Hamiltonian operator operating on the wave function; E represents the energy eigenvalue. With Schrödinger's equation, the electronic properties of molecules and atoms can be examined quantitatively. For a system of N particles and M nuclei, the Hamiltonian can be written as:

$$\begin{aligned} \hat{H} = & -\frac{\hbar^2}{2m_e} \sum_{i=1}^N \nabla_i^2 - \frac{\hbar^2}{2} \sum_{A=1}^M \frac{1}{M_A} \nabla_A^2 - e^2 \sum_{i=1}^N \sum_{A=1}^M \frac{Z_A}{r_{iA}} + e^2 \sum_{i=1}^N \sum_{j>i}^N \frac{1}{r_{ij}} \\ & + e^2 \sum_{A=1}^M \sum_{B>A}^M \frac{Z_A Z_B}{r_{AB}} \end{aligned} \quad (2.2)$$

In this equation, \hbar is the reduced Planck constant, $\hbar = \frac{h}{2\pi}$. m_e is the mass of an electron. M_A represents the mass of each nucleus. e is the charge of an electron. r_{ij} is the distance between electrons i and j , and, similarly, r_{AB} is the distance between nuclei A and B . Z_A and Z_B are the atomic numbers of each atom in the system, so they represent the number of protons in each atom's nucleus. ∇ is the vector differential operator (also called “del” or “nabla”), where, in three dimensions:

$$\nabla = \frac{\partial}{\partial x_q} + \frac{\partial}{\partial y_q} + \frac{\partial}{\partial z_q} \quad (2.3)$$

The form ∇^2 represents the Laplacian operator, which is the divergence of the gradient of a function, so:

$$\nabla^2 = \frac{\partial^2}{\partial x_q^2} + \frac{\partial^2}{\partial y_q^2} + \frac{\partial^2}{\partial z_q^2} \quad (2.4)$$

The notation of equation (2.2) can be simplified by switching to atomic units. In atomic units (specifically, Hartree atomic units), the fundamental physical constants in the above equation (m_e, e, \hbar), in addition to the Coulomb's constant ($\frac{1}{4\pi\epsilon_0}$), are all set to unity. This yields the fundamental unit of length to be the Bohr (also referred to as the Bohr radius), defined as $a_0 = \frac{4\pi\epsilon_0}{m_e e^2}$, where $1 a_0 = 5.2918 \times 10^{-11} m$. In addition, the fundamental unit of energy is the Hartree (E_h), defined as $E_h = \frac{\hbar^2}{m_e a_0^2}$, where $1 E_h = 2 \text{ Rydberg} = 27.21 \text{ eV}$. Equation (2.2) expressed in atomic units is:

$$\hat{H} = -\frac{1}{2} \sum_{i=1}^N \nabla_i^2 - \frac{1}{2} \sum_{A=1}^M \frac{1}{M_A} \nabla_A^2 - \sum_{i=1}^N \sum_{A=1}^M \frac{Z_A}{r_{iA}} + \sum_{i=1}^N \sum_{j>i}^N \frac{1}{r_{ij}} + \sum_{A=1}^M \sum_{B>A}^M \frac{Z_A Z_B}{r_{AB}} \quad (2.5)$$

The first term on the right hand side of equation (2.5) represents the kinetic energy, T , of the N electrons of the system. The second term is the kinetic energy, T , of the M nuclei of the system. The third term represents V_{Ne} , potential energy from the attractive electrostatic interactions

between nuclei and electrons. The fourth term V_{ee} represents potential energy from the repulsive electrostatic interactions between electrons. And finally, the fifth term V_{NN} represents potential energy associated with the repulsive interactions between nuclei.

As is apparent in equation (2.5), anything other than the simplest of systems will quickly become unwieldy and too complex to solve. For instance, a $LiCoO_2$ molecule has 38 electrons and four nuclei (so $N = 38, M = 4$). When this equation is applied to that molecule and the summations are expanded, it will yield 1,654 individual terms. Clearly, approximations and simplifications are required.

2.1 Born-Oppenheimer Approximation

One such simplification is the Born-Oppenheimer (BO) approximation, proposed in 1927 by Max Born and J. Robert Oppenheimer.³³ For this approximation, the core observations are that the mass of each nucleus is much larger than the mass of an electron ($M_A \gg m_e$), and that the bulky nuclei move much more slowly than the speedy electrons. The simplification fixes the positions of the nuclei in space. Therefore, their nuclear kinetic energy, the second term in equation (2.5), is zero.

$$-\frac{1}{2} \sum_{A=1}^M \frac{1}{M_A} \nabla_A^2 \rightarrow 0 \quad (2.6)$$

Furthermore, the nucleus-nucleus interaction potential is constant since the distances between nuclei (r_{ij}) are fixed. This constant in the Hamiltonian will not affect the eigen function, so it can be removed now and added back later if desired:

$$E_{total} = E_{electrons} + E_{nuclei} \quad (2.7)$$

Where, from equation (2.5), the nucleus-nucleus interaction potential is:

$$E_{nuclei} = \sum_{A=1}^M \sum_{B>A}^M \frac{Z_A Z_B}{r_{AB}} = constant \quad (2.8)$$

With the second and fifth terms removed, the Hamiltonian of (2.5) reduces to an expression just for electron interactions:

$$\hat{H}_{electrons} = -\frac{1}{2} \sum_{i=1}^N \nabla_i^2 - \sum_{i=1}^N \sum_{A=1}^M \frac{Z_A}{r_{iA}} + \sum_{i=1}^N \sum_{j>i}^N \frac{1}{r_{ij}} \quad (2.9)$$

Since this is the equation that will be considered for the remainder of this section, for the sake of simplicity, the “electrons” subscript will not be carried forward.

The BO approximation is valuable for removing two summation terms, yet this equation yields an exact solution only for a single-electron system. A system with multiple electrons quickly becomes a computational challenge. Revisiting the $LiCoO_2$ molecule, this equation still contains 1,634 terms once the summations are expanded.

2.2 Hartree Approximation

The next significant simplification was proposed by Douglas R. Hartree in 1928.³⁴ Observing that a one-electron problem could be solved, whereas anything more complex could not, Hartree suggested that a single N -electron Schrodinger equation could be replaced with N one-electron Schrodinger equations. The Hamiltonian can be generally expressed as:

$$\hat{H} = \sum_{i=1}^N \hat{h}(i) \quad (2.10)$$

Specifically, the Hamiltonian of (2.9) becomes:

$$\hat{H} = \sum_{i=1}^N \left[-\frac{1}{2} \nabla_i^2 - \sum_{A=1}^M \frac{Z_A}{r_{iA}} + \sum_{j>i}^N \frac{1}{r_{ij}} \right] \quad (2.11)$$

It is assumed that the electrons do not interact with each other, so the resulting wave function, referred to as the Hartree product wave function, is simply the product of the one-electron wave functions.

$$\Psi^{HP}(x_1, x_2, \dots, x_N) = \chi_1(x_1) \chi_2(x_2) \dots \chi_N(x_N) \quad (2.12)$$

In this equation, x_i is the position and χ_i is the spin orbital of the i^{th} electron. The corresponding Hartree eigenvalue equation is:

$$h(i)\chi_j(x_i) = \varepsilon_j\chi_j(x_i) \quad (2.13)$$

The Schrodinger equation with eigenvalue E is:

$$H\psi^{HP} = E\psi^{HP} \quad (2.14)$$

ψ^{HP} is the Hartree product wave function.

The eigenvalue E is the sum of spin orbital energies from the one-electron systems' solutions:

$$E = \varepsilon_1 + \varepsilon_2 + \cdots + \varepsilon_N \quad (2.15)$$

The Hartree method treats each electron as moving independently of the others; an electron's motion is not correlated to other electrons. However, each electron is influenced by the potential energy of the others. Advantages of the Hartree approximation are that an unsolvable N -electron system is replaced by N solvable one-electron systems. It provides a good approximation for small atoms, like helium. However, with the approximation, the Hartree product wave functions violate the anti-symmetry principle and the Pauli Exclusion Principle.

2.3 Hartree-Fock Method

Soon after Hartree published his initial approximation method, Vladimir Fock proposed an improvement.³⁵ The Hartree method wrote the overall wave function as a product of individual, one-electron wave functions, but this product is only possible if the electrons' motion is not

correlated. Fock proposed applying the variational principle to an antisymmetric combination of N one-electron wave functions, through the use of a Slater determinant.³⁶

$$\Psi_{SD}(x_1, x_2, \dots, x_N) = \frac{1}{\sqrt{N!}} \begin{vmatrix} \chi_1(x_1) & \chi_2(x_1) & \dots & \chi_N(x_1) \\ \chi_1(x_2) & \chi_2(x_2) & \dots & \chi_N(x_2) \\ \vdots & \vdots & \ddots & \vdots \\ \chi_1(x_N) & \chi_2(x_N) & \dots & \chi_N(x_N) \end{vmatrix} \quad (2.16)$$

As in the previous section, each $\chi_i(x_i)$ term is the spin orbital of the i^{th} electron. The $\frac{1}{\sqrt{N!}}$ term is the normalization factor.

The Slater determinant of equation (2.16) resolves the most significant issues with the Hartree method. First, it accounts for anti-symmetry of the interchange of electron positions:

$$\Psi_{SD}(x_i, x_j) = -\Psi_{SD}(x_j, x_i) \quad (2.17)$$

Fock's adjustment accounted for the compulsory anti-symmetry of the wave function.

Second, if two electrons have identical spin orbitals, the result of the determinant is zero.

Hartree-Fock disallows two electrons of identical spin occupying the same location, thus adhering to the Pauli Exclusion Principle. The Hartree method did not account for the Exclusion Principle. Whereas the Hartree method assumed electrons moved independently of each other in every way, the Hartree-Fock method corrected for both anti-symmetry and the Exclusion Principle.

The Hartree-Fock eigenvalue equation is:

$$f(i)\chi_j(x_i) = \varepsilon_i\chi_j(x_i) \quad (2.18)$$

In this equation, $f(i)$ is the Fock operator and has the form:

$$f(i) = -\frac{1}{2}\nabla_i^2 - \sum_{A=1}^M \frac{Z_A}{r_{iA}} + V^{HF}(i) \quad (2.19)$$

The $V^{HF}(i)$ operator is the Hartree-Fock Potential. It is the average repulsive potential on the i^{th} electron from all the other electrons in the system. Recall equation (2.9):

$$\hat{H} = -\frac{1}{2}\sum_{i=1}^N \nabla_i^2 - \sum_{i=1}^N \sum_{A=1}^M \frac{Z_A}{r_{iA}} + \sum_{i=1}^N \sum_{j>i}^N \frac{1}{r_{ij}} \quad (2.9)$$

In anything but the simplest of systems, the third term in equation (2.9) is the most complex and accounts for the most terms (N^2 terms). This term can now be simplified with the one-electron Hartree-Fock potential, $V^{HF}(i)$:

$$V^{HF}(i) = \sum_j^N [J_i(x_i) - K_j(x_i)] \quad (2.20)$$

...where J is the Coulomb operator and K is the exchange operator. Therefore, the total energy of the Hartree-Fock approximation is expressed as:

$$E_{HF} = \langle \Psi_{SD} | H | \Psi_{SD} \rangle \quad (2.21)$$

So, let ε_i represent a single electron's nuclear interactions plus the electron's kinetic energy, where (from equation (2.9)):

$$\varepsilon_i = \int \chi_i^*(x_i) \left(-\frac{1}{2} \nabla^2 - \sum_A \frac{Z_A}{r_{iA}} \right) \chi_i(x_i) dx_i \quad (2.22)$$

For reference, bracket definitions are as follows:

$$\begin{aligned} \langle i|h|j \rangle &= h_{ij} \\ &= \langle i|h|j \rangle \\ &= \int dr_i \psi_i^*(r_i) h \psi_j(r_j) \end{aligned} \quad (2.23)$$

...and...

$$\begin{aligned} \langle ij|h|kl \rangle &= \langle \psi_i \psi_j | \psi_k \psi_l \rangle \\ &= \iint dr_i dr_j \frac{\psi_i^*(r_i) \psi_j(r_i) \psi_k^*(r_j) \psi_l(r_j)}{r_{ij}} \end{aligned} \quad (2.24)$$

Define the Coulomb integral, J_{ij} , as:

$$J_{ij} = \langle ii|jj \rangle = \iint dx_i dx_j \frac{|\chi_i(x_i)|^2 |\chi_j(x_j)|^2}{r_{ij}} \quad (2.25)$$

Define the exchange integral, K_{ij} , as:

$$K_{ij} = \langle ij|ji \rangle = \iint dx_i dx_j \frac{\chi_i^*(x_i) \chi_j^*(x_j) \chi_j(x_i) \chi_i(x_j)}{r_{ij}} \quad (2.26)$$

Hartree-Fock (HF) energy is:

$$E_{HF} = \sum_{i=1}^N \varepsilon_i - \frac{1}{2} \sum_{i=1}^N \sum_{j=1}^N (J_{ij} - K_{ij}) \quad (2.27)$$

HF energy expressed in terms of the Slater Determinant:

$$E_{HF} = \sum_{i=1}^N \varepsilon_i - \langle \Psi_{SD} | V_{ee} | \Psi_{SD} \rangle \quad (2.28)$$

Fock's refinement to the Hartree Method resolves the anti-symmetry principle and Pauli's Exclusion Principle that were violated in the original approximation. Furthermore, the HF method improves accuracy of the approximation by expressing the Coulomb and exchange terms. However, because there is just a single Slater determinant, each electron interacts with just the average potential of the other electrons. A more accurate method, called Configuration Interaction (CI), accounts for the interactions of each electron pair with a Slater determinant for each pair in a linear combination. In addition, there are other methods, referred to as Post-Hartree-Fock methods, that take the HF method and perform additional calculations to address

deficiencies like electron-electron repulsion. Because of electron-electron integrals in both the Coulomb and exchange terms, the HF method quickly becomes computationally intensive with more complex systems. Adding more precision to the calculations of the electron configurations, Post-HF and CI methods demand even more computational effort and are therefore limited to smaller systems, like small molecules and molecular clusters.

2.4 Density Functional Theory

In 1964, Pierre Hohenberg and Walter Kohn published a method that would serve as the foundation for solving many-body systems that had previously overwhelmed Schrodinger's wave function. This new method is centered on defining an electronic density instead of relying on a many-body wave function. The immediate benefit is apparent when the number of variables is considered. Factoring in spatial coordinates, a wave function of N electrons has $3N$ variables. However, density is a function of only the three spatial coordinates. The advantages of using density were recognized in the early days of quantum mechanics, but the results were too inaccurate to be widely adopted. For instance, in 1927, Llewellyn Thomas and Enrico Fermi proposed a method for expressing an electronic system's kinetic energy as a function of the electron density. Improvements to Thomas-Fermi methods were made in the coming years by Paul Dirac and Carl Friedrich von Weizsäcker, but because kinetic energy makes up a large part of a system's overall energy, inaccuracies in the representation of kinetic energy amplify to significant shortcomings in the method. Particularly, resultant energies are not accurate, and bonding between atoms is not predicted.

2.4.1 Hohenberg-Kohn Formulation

Hohenberg and Kohn's breakthrough is based on two theorems. The first states that the external potential, $V_{ext}(r)$, and consequently also the total energy, of a system is a unique functional of the electron density. The variational principle in mathematical terms is:

$$E = \frac{\langle \psi | H | \psi \rangle}{\langle \psi | \psi \rangle} \geq E_0 \quad (2.29)$$

The second theorem forwarded by Hohenberg and Kohn in 1964 states that the total energy functional is minimized only by the exact ground state density. The effect of these theorems is that in finding a solution to a quantum mechanical system, the objective is shifted away from solving a many-body Schrodinger equation, and the focus is now to minimize a density functional.

Ground state energy expressed as a functional of electron density is:

$$E[\rho] = T[\rho] + E_{ee}[\rho] + \int dr \rho(r) V_{ext}[\rho] \quad (2.30)$$

In this equation, the third term represents the contribution from the external potential, and it varies depending on the actual system. $T[\rho]$ and $E_{ee}[\rho]$ are kinetic energy and repulsive inter-electron energy, respectively, both functionals of electron density, and together, they represent the Hohenberg-Kohn functional:

$$\begin{aligned}
F_{HK}[\rho] &= T[\rho] + E_{ee}[\rho] \\
F_{HK}[\rho] &= \langle \psi | \hat{T} + \hat{V}_{ee} | \psi \rangle
\end{aligned}
\tag{2.31}$$

The Hohenberg-Kohn functional is independent of the actual system, although its exact form is not known. The inter-electron term can be expressed as:

$$E_{ee}[\rho] = J[\rho] + E_{non-class}[\rho] \tag{2.32}$$

Where the Coulomb integral, $J[\rho]$, is:

$$J[\rho] = \frac{1}{2} \int dr_1 dr_2 \frac{\rho(r_1)\rho(r_2)}{|r_1 - r_2|} \tag{2.33}$$

The $E_{non-class}[\rho]$ term is a combination of self-interaction, exchange, and correlation corrections.

The total energy expression is:

$$E[\rho] = T[\rho] + J[\rho] + E_{ext}[\rho] + E_{xc}[\rho] \tag{2.34}$$

In this equation, $T[\rho]$ is the kinetic energy of the electrons. $J[\rho]$ is the coulombic repulsion between electrons. $E_{ext}[\rho]$ is the coulombic attraction between electrons and nuclei:

$$E_{ext}[\rho] = \int V_{ext}(r)\rho(r)dr \tag{2.35}$$

Where:

$$V_{ext} = \sum_A \frac{Z_A e^2}{|r - R_A|} \quad (2.36)$$

$E_{xc}[\rho]$ is the exchange and correlation energy, correcting for electrons with identical spins (exchange, E_x) for electrons with different spins (correlation, E_c). It also corrects for non-classical self-interaction effects.

$$\begin{aligned} E_{xc}[\rho] &= E_x[\rho] + E_c[\rho] \\ &= \int \rho(r) \varepsilon_x dr + \int \rho(r) \varepsilon_c dr \end{aligned} \quad (2.37)$$

Note that exchange energy is always greater than correlation energy:

$$E_x > E_c \quad (2.38)$$

2.4.2 Local Density Approximation

A goal for achieving good solutions in DFT is to improve the approximation for the exchange-correlation energy functional, $E_{xc}[\rho]$. A basic approximation technique, called the Local Density Approximation (LDA), establishes that the electrons in the system form a homogeneous gas and derives its name from the observation that the functional depends only on the position where the density being evaluated. The simplest version of this assumes that electron density, ρ_0 , is constant. This very simply makes the exchange-correlation energy:

$$E_{xc} = N \varepsilon_{xc}(\rho_0) \quad (2.39)$$

Where $\varepsilon_{xc}(\rho_0)$ is the exchange-correlation energy for each electron. Since N is:

$$N = \int d^3r \rho_0 \quad (2.40)$$

Exchange-correlation energy can be expressed as an integral over the entire volume of the uniform gas:

$$E_{xc} = \int d^3r \rho_0 \varepsilon_{xc}(\rho_0) \quad (2.41)$$

A better LDA approximation, proposed by Kohn and Sham³⁷, considers the electron gas to be changing slowly over gradual changes in position, making electron density, $\rho(\vec{r})$, a function of position, r . The integral to find the exchange-correlation energy is:

$$E_{xc} = \int d^3r \rho(\vec{r}) \varepsilon_{xc}[\rho(\vec{r})] \quad (2.42)$$

The exchange energy for each particle is:

$$\varepsilon_x = -\frac{3}{4} \left(\frac{3}{\pi} \right)^{1/3} \left[\rho(\vec{r}) \right]^{1/3} \quad (2.43)$$

Therefore, the expression for exchange energy is:

$$E_x^{LDA} = -\frac{3}{4} \left(\frac{3}{\pi} \right)^{1/3} \int d^3r \rho(\vec{r})^{4/3} \quad (2.44)$$

And the exchange potential is:

$$\begin{aligned} V_x^{LDA} &= \frac{\partial E_x^{LDA}}{\partial \rho} \\ &= -\left(\frac{3}{\pi} \right)^{1/3} [\rho(\vec{r})]^{1/3} \end{aligned} \quad (2.45)$$

This technique can work suitably well for systems with small, gradual variations like a pure, ideal metal. It is not adequate to analyze atomic or molecular systems and yields inaccurate results for even the H atom. LDA tends to slightly underestimate exchange energy by about 10% but overestimates correlation energy by 200%. It also over-binds particles, estimating bond lengths to be too short and making phonon bonds too stiff. LDA is a spin-unpolarized technique. A variation, Local Spin Density Approximation (LSDA), includes electron spin.

2.4.3 Generalized Gradient Approximation

Functionals for the Generalized Gradient Approximation (GGA) depend both on density, ρ , and on the gradient of density, $\nabla\rho$. This addresses the issue with LDA of not handling density that changes quickly with position and makes GGA better suited for inhomogeneous densities, like molecules and atoms. Exchange-correlation energy with the gradient correction is:

$$E_{xc}^{GGA} = E_{xc}[\rho(\vec{r}), \nabla\rho(\vec{r})] \quad (2.46)$$

GGA results in more accurate atomic and molecular energies than LDA. It also estimates bonding more accurately.

2.4.4 Hybrid Functionals

There are advantages and disadvantages to the various methods and approximations. The Hartree-Fock method yields the exact exchange energy but overestimates bond energies and underestimates bond lengths. GGA underestimates bond energies and overestimates bond lengths. Fractionally combining HF with various DFT methods offers the opportunity to tune the overall method based on experimental observations. One such hybrid functional that appears to be the ubiquitous example across DFT review literature is the B3LYP functional. This was published in 1988 by A. D. Becke, and it includes three semi-empirical parameters to combine: 1) exchange energies from HF and LDA (E_x^{HF}, E_x^{LDA}); 2) Becke's GGA exchange correction (ΔE_x^{B88}); 3) Vosko-Wilk-Nusair LDA correlation functional (E_c^{VWN}); and 4) correlation energies from Lee, Yang, and Parr's GGA correlation functional (E_c^{LYP}). The name, B3LYP, derives from: Becke, three parameter, Lee-Yang-Parr. The B3LYP hybrid functional is:

$$E_{xc}^{B3LYP} = E_x^{LDA} + a_0(E_x^{HF} - E_x^{LDA}) + a_x\Delta E_x^{B88} + E_c^{VWN} + a_c(E_c^{LYP} - E_c^{VWN}) \quad (2.47)$$

In this equation, a_0 , a_x , and a_c are the parameters found by fitting with empirical data, where $a_0 = 0.20$, $a_x = 0.72$, $a_c = 0.81$.

Another hybrid functional is BPW91. It combines Becke's exchange functional with a correlation functional published by Perdew and Wang in 1991.³⁸

2.4.5 Basis Sets

When computing DFT calculations, a set of functions is specified to represent the molecular orbitals. The overall molecular orbitals, Ψ_i are represented as a linear combination of single-electron orbitals, χ_μ , expressed as:

$$\Psi_i = \sum_{\mu=1}^N C_{\mu i} \chi_\mu \quad (2.48)$$

In this equation, $C_{\mu i}$ represents the molecular expansion coefficients, and χ_μ is the μ^{th} one-electron orbital out of N total atomic orbitals. The two main types of orbitals are Slater-Type Orbitals (STO) and Gaussian Type Orbitals (GTO). STOs employ spherical harmonics to decay exponentially from the atomic nucleus, and they are good representational functions of actual electron orbitals. However, they are computationally intense. GTOs, on the other hand, are less computationally expensive but also, individually, are lower fidelity than STOs. Particularly, GTOs fail for small radii, where they have a slope of zero instead of cusping down, as expected. GTOs are expressed as:

$$\chi(x, y, z) = N x^{l_x} y^{l_y} z^{l_z} e^{-\xi r^2} \quad (2.49)$$

In this equation, l_x , l_y , and l_z are the angular components of the orbital, and ξ is the radial component.

Assembling a linear combination of GTOs improves their accuracy. To approach the accuracy of a set of STOs, approximately three times as many GTOs are required. A linear combination of GTOs to stand in for a single basis function is called a contracted Gaussian function (CGF).

They have the form:

$$\chi_{\mu}^{CGF} = \sum_{i=1}^L d_{i\mu} \chi_i^{GF}(\xi_{i\mu}, r) \quad (2.50)$$

In this equation, χ_{μ}^{CGF} is the CGF, and χ_i^{GF} is the primitive GTO. $d_{i\mu}$ represents the contraction coefficients, L is the length of the contraction, and $\xi_{i\mu}$ represents the contraction exponents.

Basis sets are expressed in a series of specific numbers and characters. The numbers indicate how many GTOs comprise each orbital. An example of a minimal basis set is STO-nG, which consists of n primitive GTOs to fit a single STO. For instance, STO-3G is a linear combination of three primitive GTOs to mimic an STO. A more complex example is the split valence double-zeta basis set in the form x-yzG, where x is the number of primitive GTOs in linear combination representing the core orbitals. y and z indicate that the valence orbitals are each composed of two sets of functions, one set with y primitive GTOs and the other with z primitive GTOs. A specific example is the 3-21G basis set, with three GTOs for the core orbitals, and a pair of functions for the valence orbitals (because there are two numbers after the dash), one with two GTOs and the

other with a single GTO. There are also triple-zeta and quadruple-zeta basis sets, indicated by three and four numbers, respectively, after the dash. Characters can also be used in the basis set label for specific meaning. An asterisk (*) indicates the inclusion of polarization functions, which can help accurately predict chemical bonding. A plus sign (+) indicates the inclusion of diffuse functions, which improves the accuracy of systems that have diffuse, long distance electron densities, like anions.

3. Methods and Results

3.1 Overview

Research into LIBs has been on-going for decades, and in recent years, astonishing advances have been made in their materials, design, and, ultimately, performance. The purpose of this work is to explore the theories and methods that serve as the foundation for much of the research into the atomic clusters that have advanced the field.

In-depth understanding of atomic systems involves solving Schrodinger's equation. However, as discussed above, for any but the simplest systems, this is intractable. The research carried out in this thesis is based on Density Functional Theory (DFT) because DFT enables a quantitative treatment of a relatively complex system and it is computationally practical.

DFT has been extensively used to study the properties of existing electrolytes and predict new ones. It was discovered that the negative ion components of electrolytes are superhalogens, i.e. their electron affinities are larger than that of a halogen atom. Considerable amount of work on superhalogens exists in the literature and ideas generated from these studies enabled researchers to predict new electrolytes whose negative ion components do not contain toxic halogens as do the current electrolytes. This prediction has been experimentally confirmed.³⁹ The objective in this thesis was to examine the properties of current cathode materials and see if the ideas developed in cluster science can similarly be used to design better cathode materials. Using DFT and the Gaussian G03 software, the properties of various cathode materials have been studied in

this work. The electronic properties focused on for this work are the electron affinity and vertical detachment energy of the negative ion components of the cathode material, and the binding energy of these anions with the Li^+ cation. Several materials currently in use in LIB cathodes are included, in addition to a few new oxide materials to see how their electronic properties might compare to current materials.

3.2 Cluster Materials and Properties

This thesis analyzes several materials by using clusters as a model. It is known that materials where bonding is ionic, clusters can serve as good models to understand their structure-property relations. Thus, investigating clusters can illuminate the science behind the materials as an entry-point to improve the performance of their systems.

Cathode materials are most often composed of transition metal oxide (TMO). The structure and chemical properties of the TMOs are crucial to the performance of the cathode. The TMOs exhibit multiple valences, which allows them to be stable when both lithiated and delithiated. Multi-valence and stability with or without lithium are requisite for electrodes of rechargeable LIBs. During discharge, the material must lithiate, changing its chemical composition to result in a stable system. The same applies to charging. The cathode must release its lithium without structural degradation and yield a stable material. Therefore, an ideal cathode must be stable both lithiated and delithiated, and it must readily undergo the chemical process in both directions.

For instance, cobalt oxide, CoO_2 , was the breakthrough cathode material for LIBs when it was first proposed for use in 1980.⁴⁰ Cobalt's outer electron structure is $3d^7 4s^2$. The high-valent Co^{IV} species bonds with two oxygen atoms to form the stable molecule CoO_2 . When lithium is intercalated within CoO_2 , the resulting $LiCoO_2$ is also stable, effectively changing the valence of Co from 4 to 5. Here, alkali metal lithium is the positive ion, and CoO_2 is the negative ion; thus, the latter can be effectively regarded as mimicking a halogen.

3.2.1 Halogens

Halogens are the elements in group 17 of the periodic table. Having two electrons in their outermost s-orbital shell and five in their outermost p-orbital shell, they are short one electron of fulfilling the octet rule. Therefore, they are highly electronegative. A halogen atom readily reacts with many other atom species to fill that outer orbital. Halogens have a particular affinity to alkali metals, which, occupying group 1 of the periodic table, have a lone electron in their outermost shell. Together, halogens and alkali metals combine for complete electron shell closure to form salts.

Assessing $LiCoO_2$ as a salt, lithium is the alkali metal and CoO_2 behaves like a halogen. In this case, the molecule CoO_2 is larger than an elemental halogen. Is the electron affinity (EA) of CoO_2 larger than that of Cl ? How is the binding energy of Li to CoO_2 different to its binding energy to Cl ? This thesis investigates these questions while adding comparative analysis for several other clusters.

3.2.2 Electron Affinity

Electron affinity is the amount of energy gained by a neutral atom when an electron is added to form an anion. An atom with positive EA indicates that it can accept an extra electron and move to a lower, more stable, energy state. The element with the highest EA is chlorine, with $EA = 3.62$ eV. The EAs of halogen atoms are higher than that of other atoms in the periodic table. Consequently, they readily bind to alkali atoms to form a salt.

3.2.3 Vertical Detachment Energy

Vertical Detachment Energy (VDE) is the difference in energy between an anion in its ground state geometry and the neutral atom or molecule in that same geometry. Effectively, VDE is the energy released when removing an electron from an anionic complex without the neutral complex relaxing to its lower energy geometry. VDE is always greater than EA and the difference provides the signature of geometry change when an electron is removed from an anion.

3.2.4 Super Halogens

Some clusters can achieve higher EA than chlorine. For instance, in 1962, Neil Bartlett was one of the first researchers to identify such a cluster. The EA of hexafluoroplatinate, PtF_6 , was estimated to be at least 7.3 eV, strong enough remove an electron from an O_2 molecule or a Xe atom.⁴¹ Recent research has identified molecules described as superelectrophilic that are capable

of forming covalent bonds at room temperature with the noble gas argon.⁴² This class of highly-electronegative molecules was given the name “superhalogen” for exceeding of the EA of chlorine. In 1981, Gutsev and Boldyrev advanced this work by noting that superhalogens take the form $MX_{(k+1)}$, where M is the core metal atom with maximum valence k .⁴³ This core atom is surrounded by $k + 1$ halogen atoms of species X . Note that the number of halogen atoms exceeds the valence of the metal atom by one, yielding an electronegative molecule. In the last decade the list of superhalogens has expanded considerably. It has been shown that a superhalogen can be formed without the benefit of a halogen atom, metal atom or both.⁴⁴ It is also not necessary to have a central atom to form superhalogens; they can be formed with a multi-nuclear core as well.

3.2.5 Binding Energy

Binding energy (E_b) is the energy required to split a molecule apart. In particular, this work considers the binding energy of a lithium cation to the negative ion component of the Li salt. Within the cathode structure, this is an important parameter as this is the energy gained when lithium is intercalated to the metal oxide during the discharge of the battery.

3.3 Results

3.3.1 Approach

Electrolytes are composed of salts, which usually contain halogens. The halogen components are the root of many of the undesirable properties of electrolytes: They are flammable, corrosive, and

poisonous. There are immediate advantages to replacing halogens with safer alternatives, and theory has shown that replacing halogens with halogen-free superhalogens may be feasible for the electrolyte in a LIB.³² This thesis considers a similar approach to see if the chemistry of the cathode materials can be understood by analyzing the binding of the *Li* ion to the metal oxide anion. In particular, we would like to see if the metal oxide components are superhalogens and, if so, can they be replaced by other metal oxides that may or may not contain a transition metal atom. This is important for the current cathode material *LiCoO*₂, where *Co* is relatively expensive. There would be advantages both in cost and sustainability if *Co* could be replaced, even partially, in LIB cathodes.

The electronic properties mentioned in the sections above are gleaned from the Gaussian G03 software. For the calculations, a critical result from G03 is the energy of a cluster. Through computational theoretical methods, the Gaussian software attempts to find a stable geometry that minimizes the energy. Sometimes, however, that energy level may belong to a local minimum. Refinements are made to the input geometries and computations are iterated with the goal of finding lower energy levels, eventually yielding ground-state clusters. This process is performed for neutrals and anions of each cluster being assessed, as well as neutrals and anions for the relevant moieties.

For instance, to compute the EA of *CoO*₂, the ground-state energies of the neutral and anionic clusters are needed. Calculations in Gaussian are performed with the BPW91 hybrid functional and the 6-311+G* basis set. Referencing the explanations of basis sets in section 2.4.5 above, the

6-311+G* basis set is a triple-zeta basis set, and it is composed of: 1) A linear combination of six GTOs for the core orbitals; 2) Three sets of functions for each valence orbital: The first set is a linear combination of three GTOs, the second set is a single GTO, the third set is a single GTO; 3) Diffuse functions; and 4) Polarization functions.

To evaluate new clusters for their suitability, their electronic properties are compared with the properties of clusters currently in use in LIB cathodes. In particular, electron affinity (EA), vertical detachment energy (VDE), and binding energy (E_b) are investigated. The goal is to assess how these properties compare for existing cathode materials and other metal oxides not currently in use in LIB cathodes. Properties of the current materials serve as the benchmarks for the proposed materials. If the EA, VDE, and E_b are comparable, then additional and more in-depth work could be undertaken to evaluate the proposed materials.

3.3.2 Optimized Geometries of Metal Oxides

A total of 14 metal oxide clusters were explored for this thesis. Nine of these have been used in production LIBs, and they are MnO_2 , FeO_2 , CoO_2 , NiO_2 , FeO_4 , CoO_4 , NiO_4 , MoO_4 , and Mn_2O_4 . The optimized geometries of their neutrals and anions were found to be as follows:

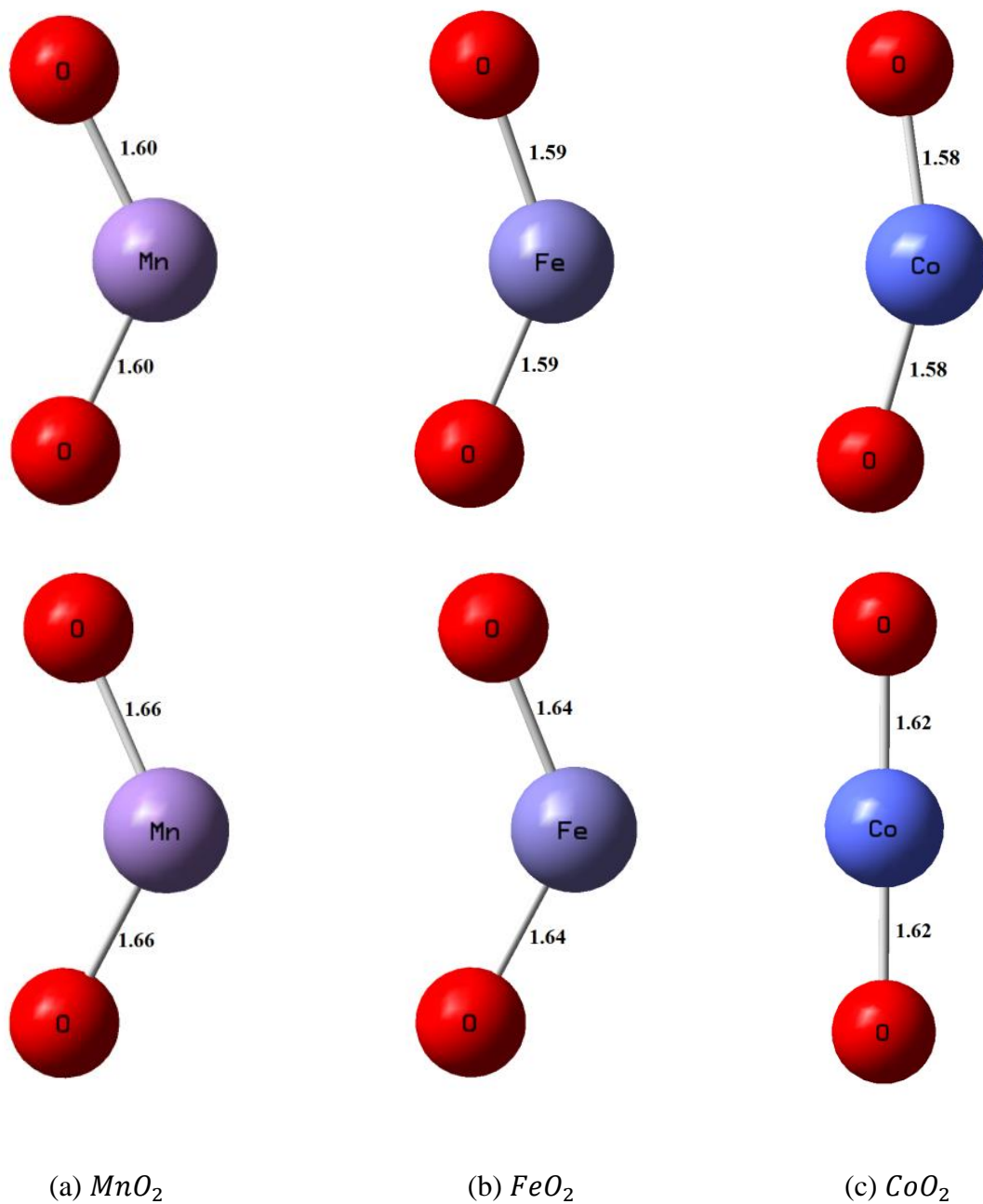


Figure 8 Optimized geometries of MnO_2 , FeO_2 , CoO_2 , with neutral on top, anion on bottom. Bond lengths in Å.

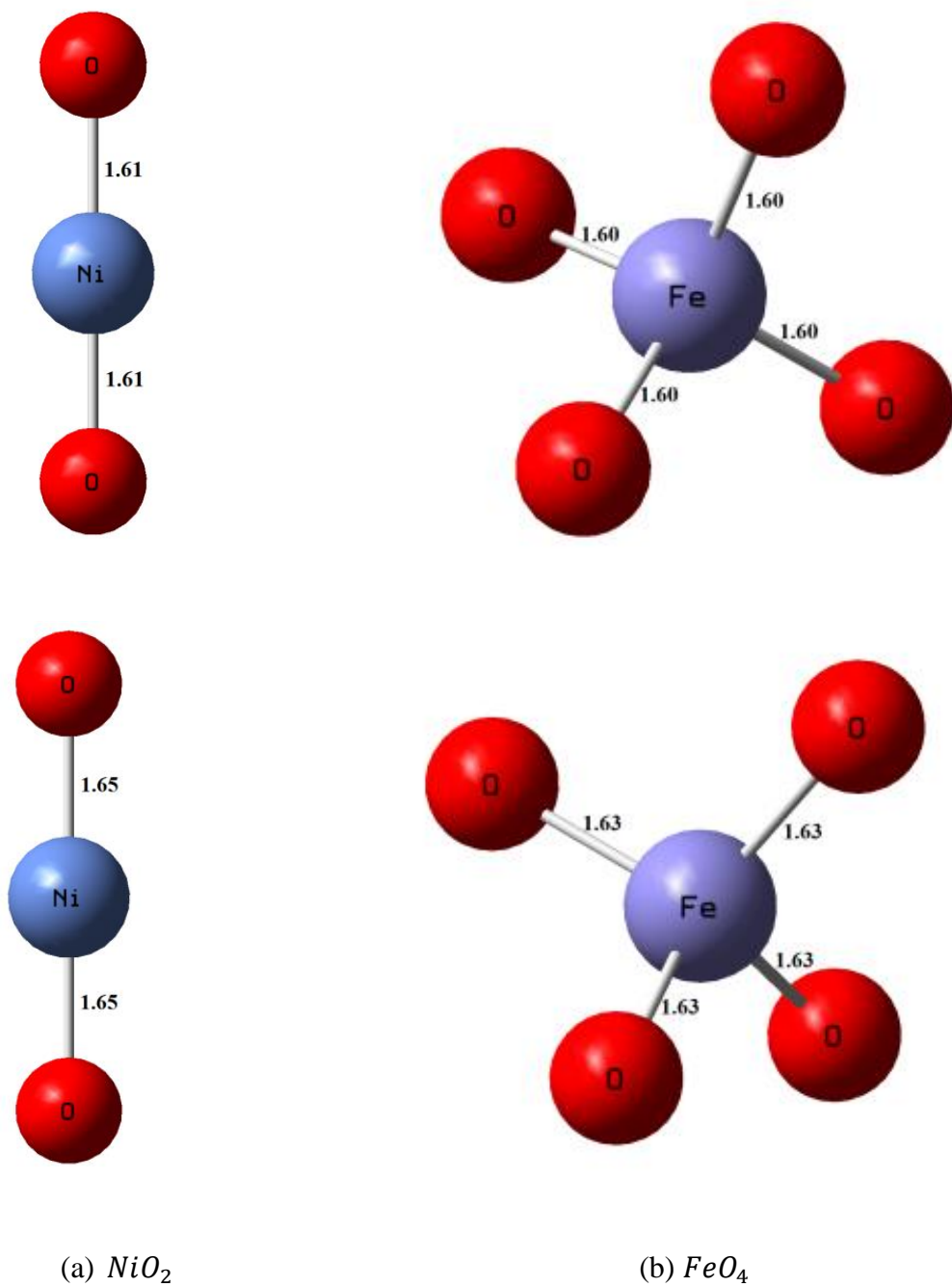
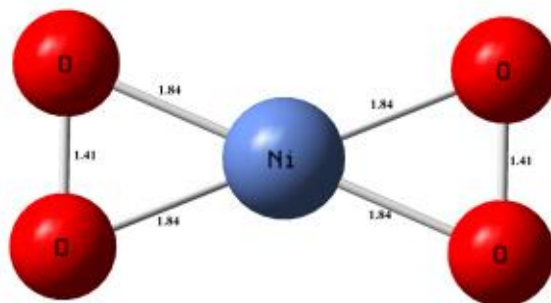
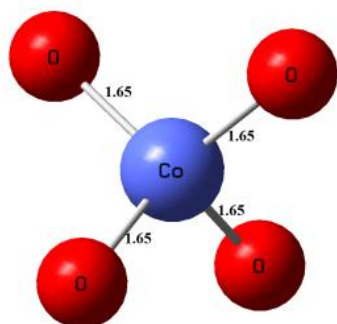
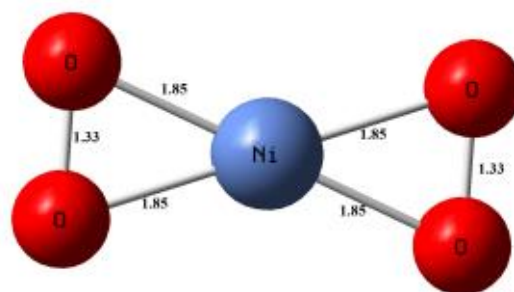
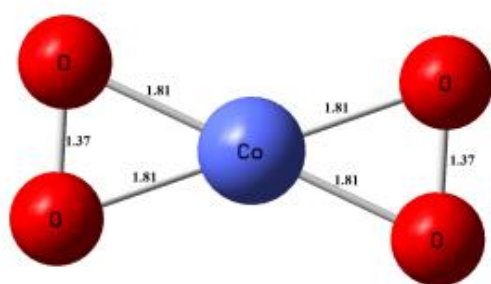


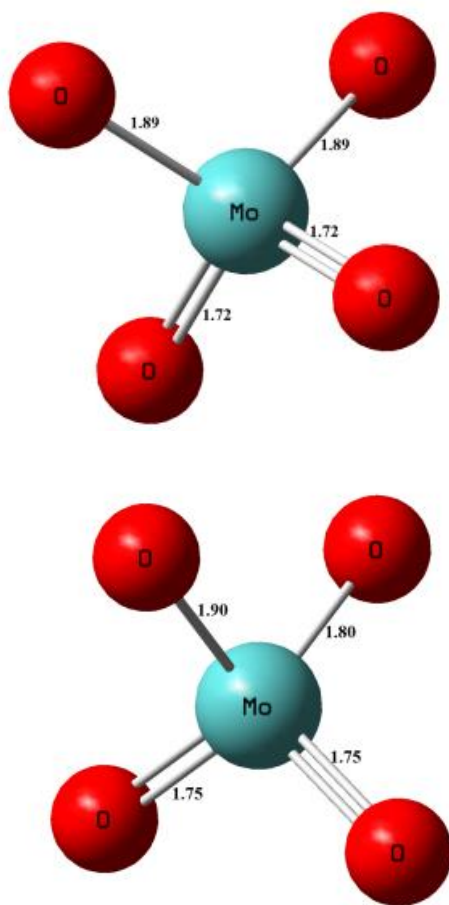
Figure 9 Optimized geometries of NiO_2 and FeO_4 , with neutral on top, anion on bottom. Bond lengths in Å.



(a) CoO_4

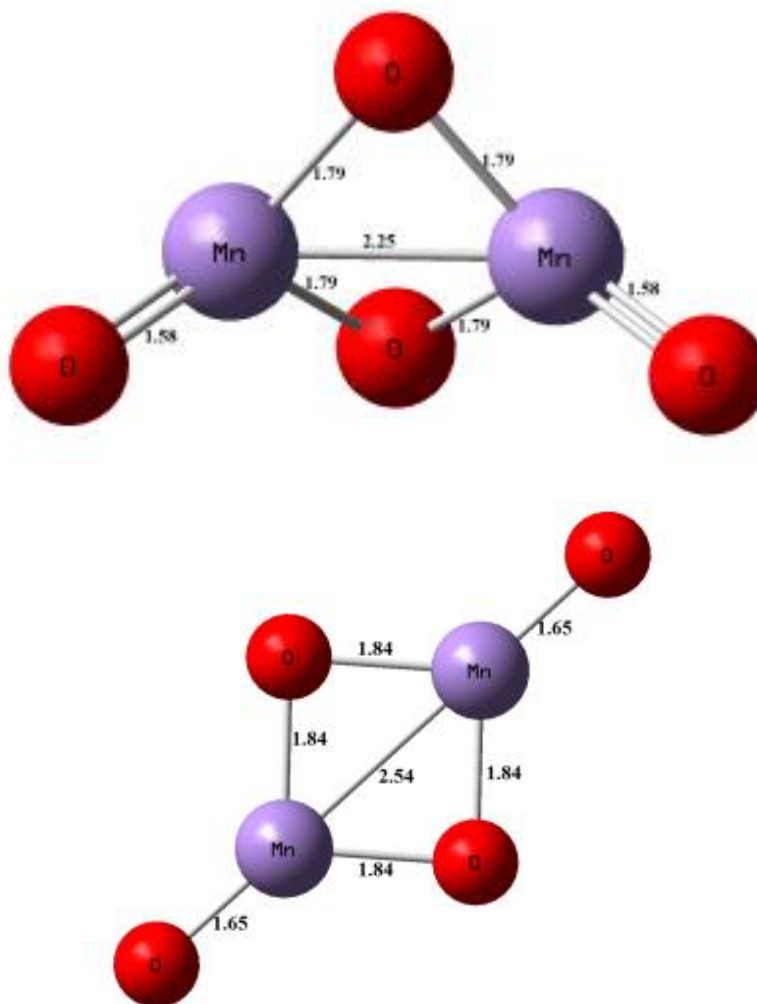
(b) NiO_4

Figure 10 Optimized geometries of CoO_4 and NiO_4 , with neutral on top, anion on bottom. Bond lengths in Å.



(a) MoO_4

Figure 11 Optimized geometries of MoO_4 , with neutral on top, anion on bottom. Bond lengths in Å.



(a) Mn_2O_4

Figure 12 Optimized geometries of Mn_2O_4 , with neutral on top, anion on bottom. Bond lengths in Å.

We note that in most cases the ground state geometries of the neutral and negative ions are similar. For these systems the VDEs and EAs do not differ significantly. These can be seen in **Table 1**.

Five molecules that are not currently used in LIBs were investigated to gain some insight into what might make a suitable replacement for the transition metal oxide in $LiCoO_2$ cathode material. These clusters are AlO_2 , VO_3 , CoO_3 , FeO_5 , and CrO_4 . The optimized geometries of the neutral and anionic clusters of these metal oxides are as follows. Again, we see that the geometries of the neutral clusters do not differ much from those of the anionic species.

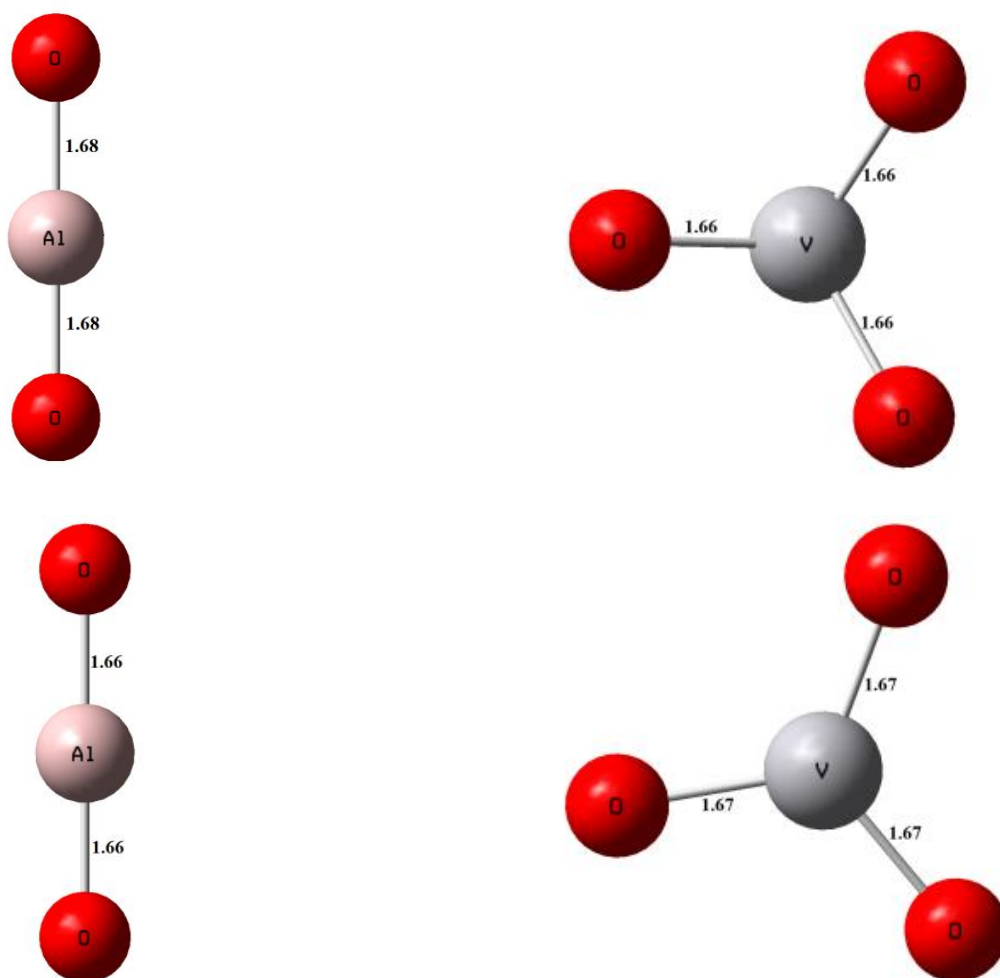


Figure 13 Optimized geometries of AlO_2 and VO_3 , with neutral on top, anion on bottom. Bond lengths in Å.

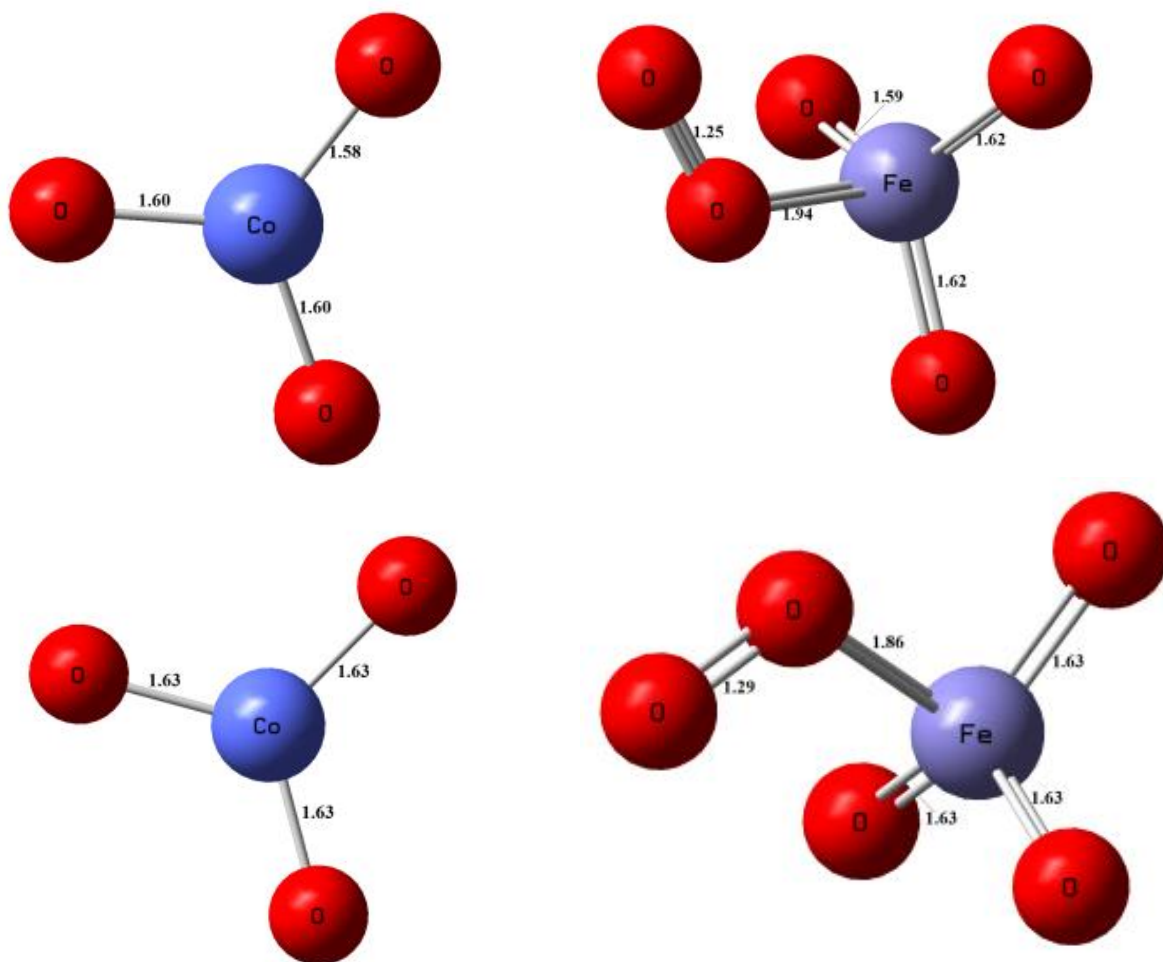


Figure 14 Optimized geometries of CoO_3 and FeO_5 , with neutral on top, anion on bottom. Bond lengths in Å.

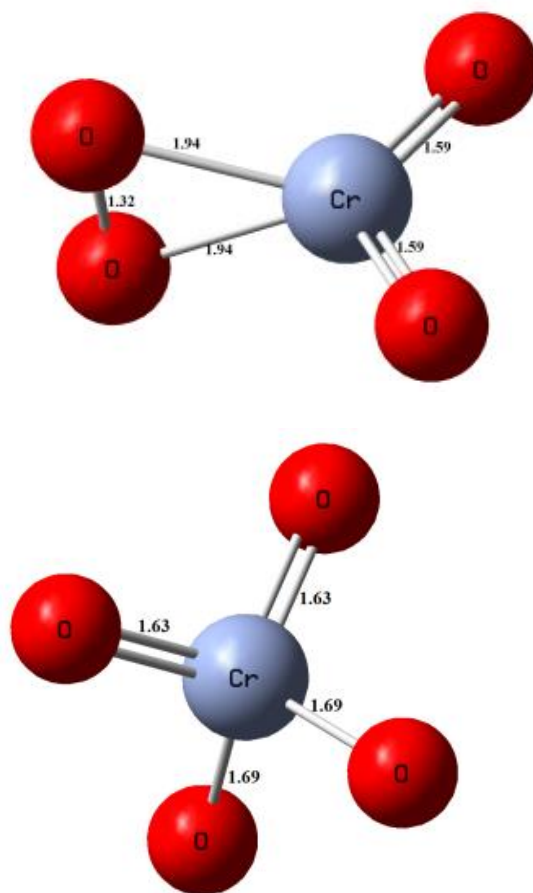


Figure 15 Optimized geometry of CrO_4 , with neutral on top, anion on bottom. Bond lengths in Å.

3.3.3 Electron Affinity and Vertical Detachment Energy

From the resulting optimized neutral and anion geometries of each cluster, EA can be calculated as follows:

$$EA = E(\text{neutral}) - E(\text{anion})$$

The vertical detachment energies (VDEs) are similarly the energy difference between the neutral and the anion where the geometry of the neutral is same as its anion. Results obtained from the modeling are given in **Table 1** and **Table 2** for the metal oxides that currently form the cathodes and the new ones we are studying.

Table 1 Electron affinity and vertical detachment energy of metal oxides currently used in cathodes. Experimental values provided when available^{45, 46}

Cluster	EA (eV)	EA exp (eV)	VDE (eV)	VDE exp (eV)
<i>MnO₂</i>	2.00	2.06	2.18	2.18
<i>FeO₂</i>	2.27	2.36	2.43	2.43
<i>CoO₂</i>	2.77	2.97	2.85	2.84
<i>NiO₂</i>	3.25	3.05	3.33	3.33
<i>FeO₄</i>	3.76	3.30	3.86	
<i>CoO₄</i>	3.80		4.65	
<i>NiO₄</i>	2.72		2.96	
<i>MoO₄</i>	5.27		5.45	
<i>Mn₂O₄</i>	2.89	2.69	3.34	

In some cases in **Table 1**, experimental results were not available. However, some theoretical results were found in other research literature. Pradhan et al. calculated EA and VDE for *CoO₄* to be 3.23 eV and 4.54 eV, respectively. EA and VDE for *NiO₄* were found to be 2.58 eV and 2.83 eV, respectively.⁴⁵ These externally predicted results favorably match the results of this research.

Computed EA of the metal oxides in established cathode materials ranges from 2.00 eV to 5.27 eV, with most of the materials in the range of 2 eV to 4 eV. For the molecules with known experimental values, the computed values compare favorably with experimental values. This

suggests the computational parameters of functional and basis set are suitable for these comparisons. Computed VDE for the established materials ranges from 2.18 eV to 5.45 eV. These are excellent matches to the known experimental values.

The EAs and VDEs of metal oxides that are proposed as possible candidates for new cathode materials are given in **Table 2**. EAs range between 3.82 and 4.68 eV, and VDEs range from 3.83 to 4.95 eV. All are within the range of VDEs for established cathode materials.

Table 2 Electron affinity and vertical detachment energy of metal oxides proposed as candidates for cathode materials. Experimental values provided when available^{45, 47, 48, 49}

Cluster	EA (eV)	EA exp (eV)	VDE (eV)	VDE exp (eV)
AlO_2	3.82	4.23	3.83	
VO_3	4.01	4.36	4.21	
CoO_3	3.97		4.07	
FeO_5	4.12		4.27	
CrO_4	4.68	4.98	4.95	5.07

As above, some experimental results were not available for **Table 2**. Pradhan et al. calculated EA and VDE for CoO_3 to be 3.89 eV and 4.04 eV, respectively.⁴⁵ Vyboishchikov et al. found the VDE of VO_3 to be 4.22.⁴⁹ Again, these external results favorably match the results of this research.

Figure 16 shows a comparison of EA values for all the investigated clusters, with the EA of CoO_2 as a benchmark. The new materials being investigated fall within the same overall range of

the established materials; however, all the new metal oxide materials have EAs greater than that of chlorine, which classifies them as superhalogens. Higher EAs suggest that the materials may bond more readily with lithium.

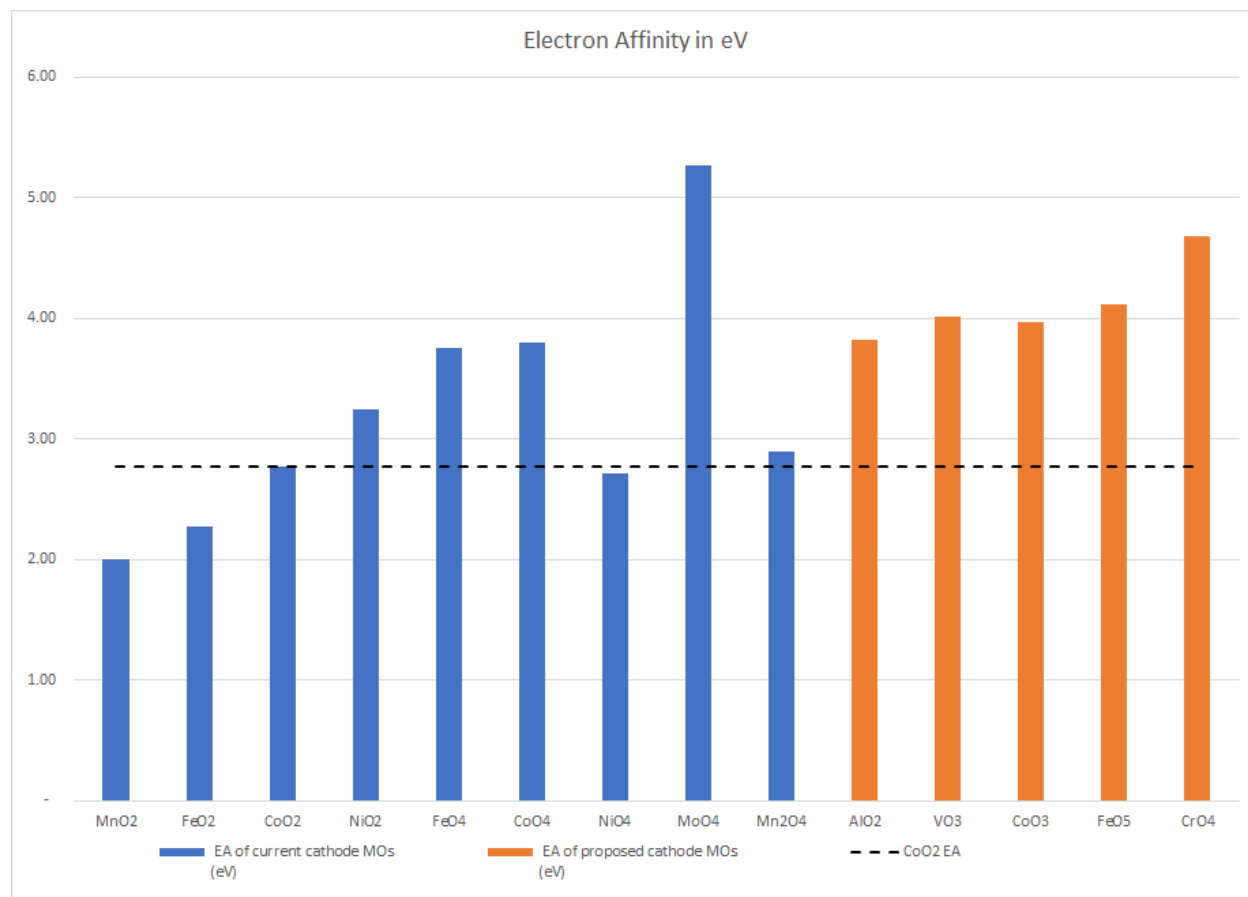


Figure 16 Electron affinities of investigated metal oxides

3.3.4 Optimized Geometries of Lithium-Bearing Salts

We next study the binding energy of Li^+ cation to the metal oxide anions discussed in the above.

A total of 16 lithium-bearing clusters were explored for this paper. Eleven of these have been

used in production LIBs, and they are $LiMnO_2$, $LiFeO_2$, $LiCoO_2$, $LiNiO_2$, $LiFeO_4$, $LiCoO_4$, $LiNiO_4$, $LiMoO_4$, Li_2MoO_4 , $LiMn_2O_4$, and $Li_2Mn_2O_4$. The geometries of these Li salts are given in the following figures. The effects of inserting the Li^+ cation can be observed in each geometry. Compared to the metal oxide geometries, oxygen atoms are angled away from more linear configurations by the Li , and metal-to-oxygen bond lengths are slightly stretched. For all but $LiMn_2O_4$ and $Li_2Mn_2O_4$, the basic geometry of the metal oxide component is preserved.

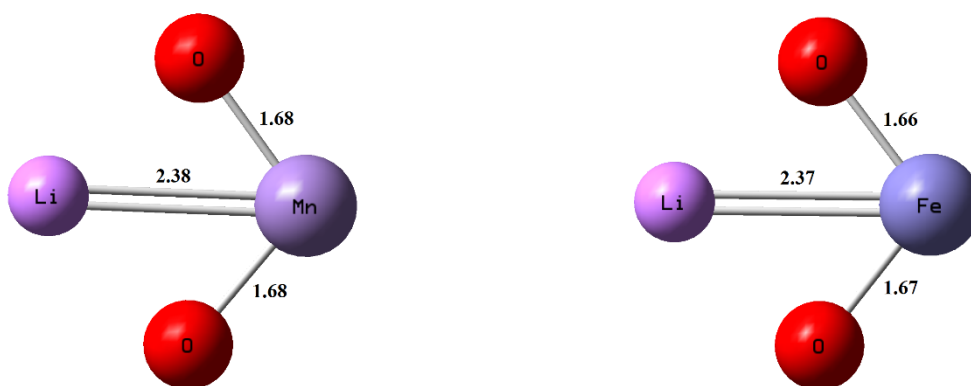


Figure 17 Optimized geometries of $LiMnO_2$ and $LiFeO_2$. Bond lengths in Å.

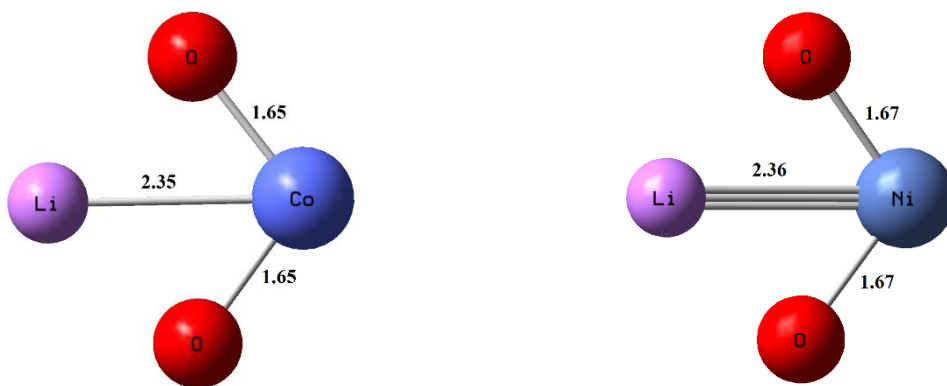


Figure 18 Optimized geometries of $LiCoO_2$ and $LiNiO_2$. Bond lengths in Å.

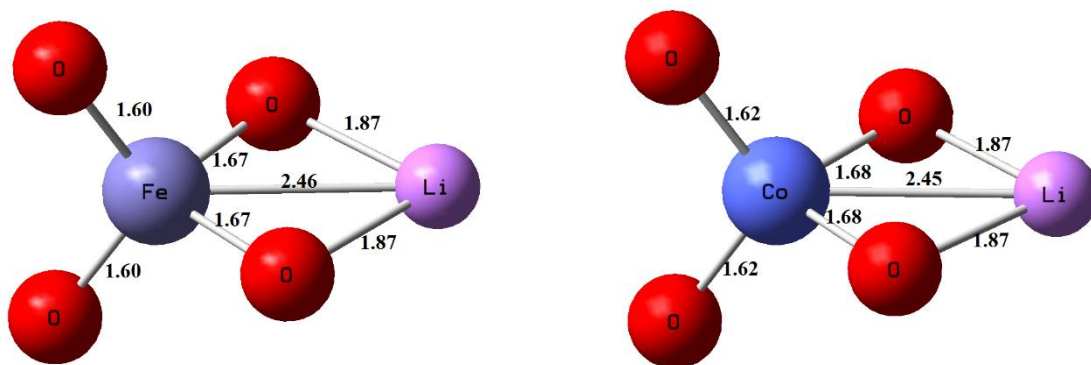


Figure 19 Optimized geometries of $LiFeO_4$ and $LiCoO_4$. Bond lengths in Å.

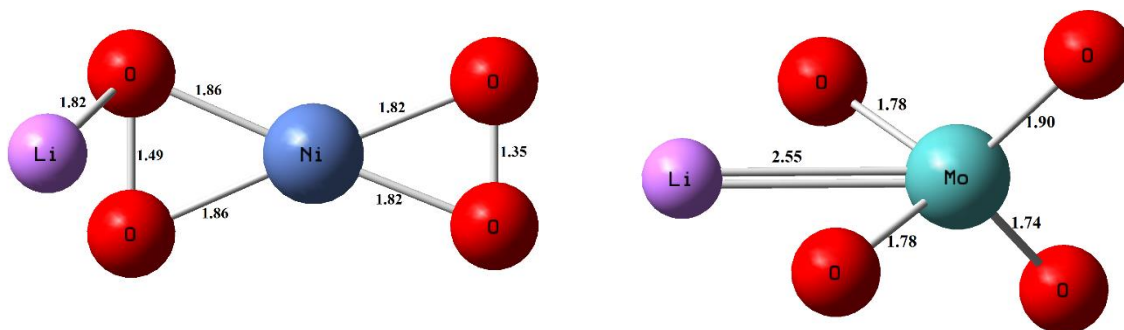


Figure 20 Optimized geometries of $LiNiO_4$ and $LiMoO_4$. Bond lengths in Å.

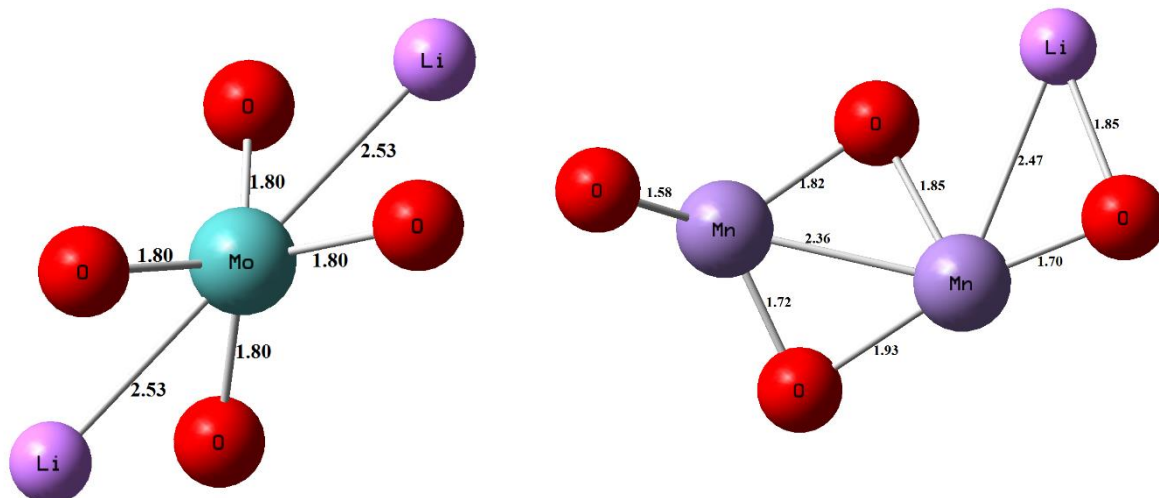


Figure 21 Optimized geometries of Li_2MoO_4 and $LiMn_2O_4$. Bond lengths in Å.

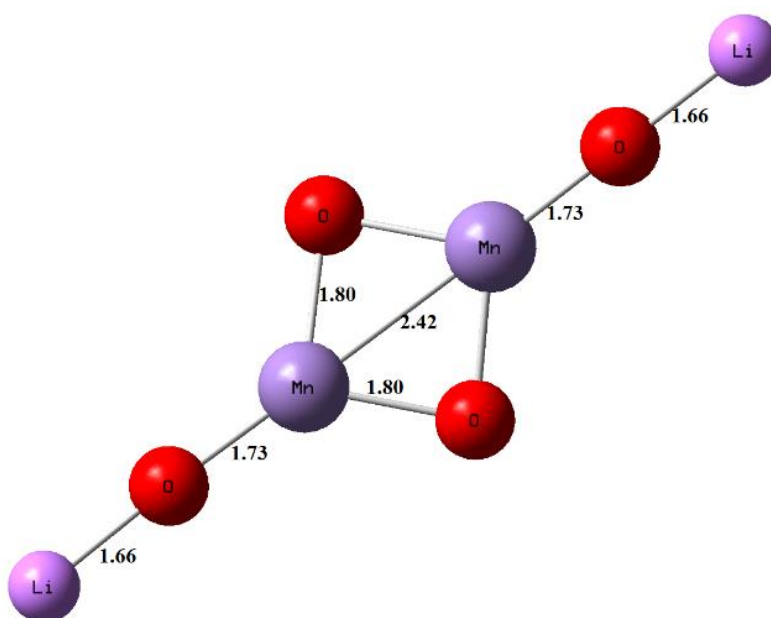


Figure 22 Optimized geometry of $Li_2Mn_2O_4$. Bond lengths in Å.

The metal oxides being proposed as possible new cathode materials are LiAlO_2 , LiVO_3 , LiCoO_3 , LiFeO_5 , and LiCrO_4 . They were modeled and optimized, and their geometries follow in the figures below. As with the clusters currently used in LIB cathodes, the metal oxide components of these clusters retain their basic geometry after lithium insertion. The oxygen atoms adjacent to the lithium are angled toward the lithium, and their bond lengths increase slightly.

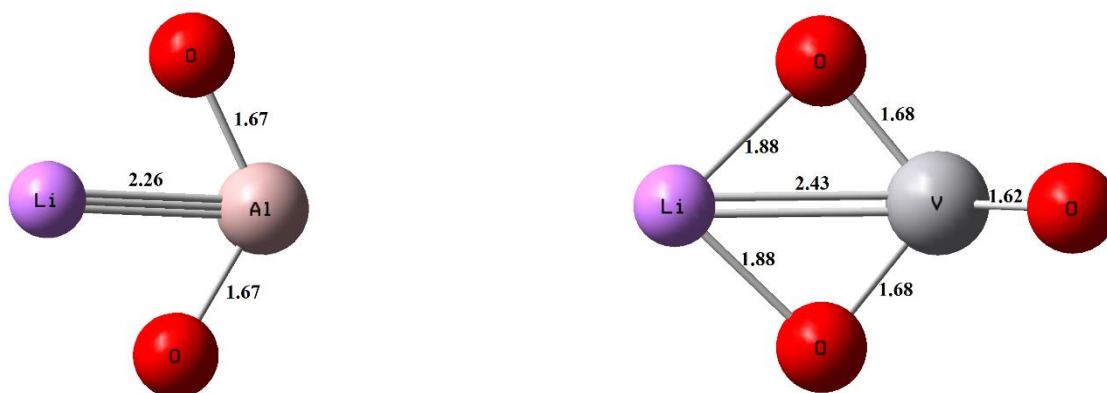


Figure 23 Optimized geometries of LiAlO_2 and LiVO_3 . Bond lengths in Å.

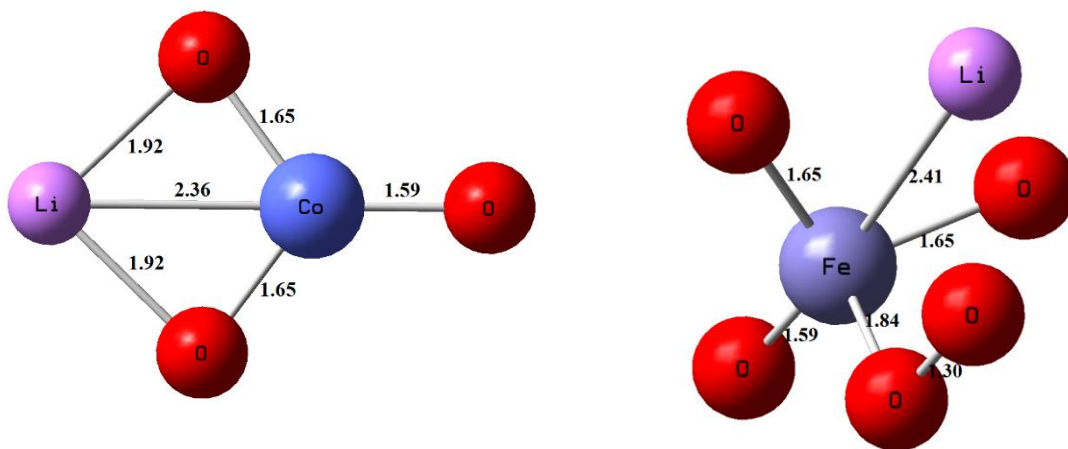


Figure 24 Optimized geometries of LiCoO_3 and LiFeO_5 . Bond lengths in Å.

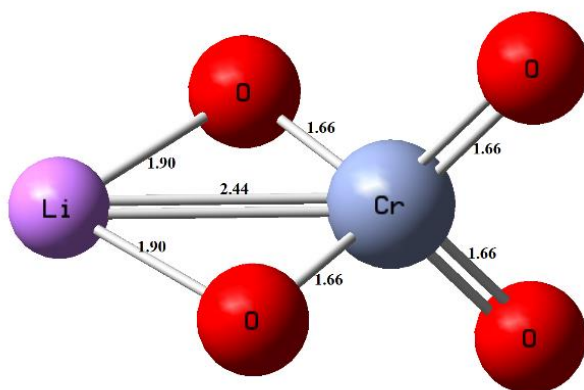


Figure 25 Optimized geometry of $LiCrO_4$. Bond lengths in Å.

3.3.5 Binding Energy

Calculating the binding energy requires optimized geometries of the salt, metal oxide anion, and the Li^+ cation. Calculations for binding energy, as they apply to this research, require ground-state energy values for a lithium cation, metal oxide anion, and the neutral of the combined salt.

For instance, binding energy is calculated for $LiCoO_2$ as follows:

$$E_b(LiCoO_2) = E(Li^+) + E(CoO_2^-) - E(LiCoO_2)$$

In effect, the binding energy is the difference between the ground state energies of the two component ions, $E(Li^+) + E(LiCoO_2^-)$, and the ground state energy of the full salt molecule, $E(LiCoO_2)$.

Binding energy for the current cathode materials was calculated to be as follows:

Table 3 Calculated binding energies (in eV) of current cathode materials

Cluster	E_b (eV)
<i>LiMnO₂</i>	7.07
<i>LiFeO₂</i>	7.01
<i>LiCoO₂</i>	6.56
<i>LiNiO₂</i>	6.52
<i>LiFeO₄</i>	6.20
<i>LiCoO₄</i>	6.13
<i>LiNiO₄</i>	6.18
<i>LiMoO₄</i>	11.49
<i>Li₂MoO₄</i>	6.92
<i>LiMn₂O₄</i>	8.88
<i>Li₂Mn₂O₄</i>	5.28

For the new cathode materials, binding energy was found to be as follows:

Table 4 Calculated binding energies (in eV) of proposed candidates for cathode materials.

Cluster	E_b (eV)
<i>LiAlO₂</i>	5.86
<i>LiVO₃</i>	6.63
<i>LiCoO₃</i>	6.17
<i>LiFeO₅</i>	6.01
<i>LiCrO₄</i>	6.07

Figure 26 shows a comparison of binding energy values with the E_b of CoO_2 as a benchmark. For the established cathode materials, binding energy ranges from 5.99 eV to 11.49 eV. The new cathode materials being investigated are on the low-end of this range, with a minimum of 5.86 eV and a maximum of 6.63 eV. Lower binding energy suggests that Li^+ will more readily be inserted and removed from the cathode material, so the new metal oxides being considered may perform better as a cathode material than those currently used.

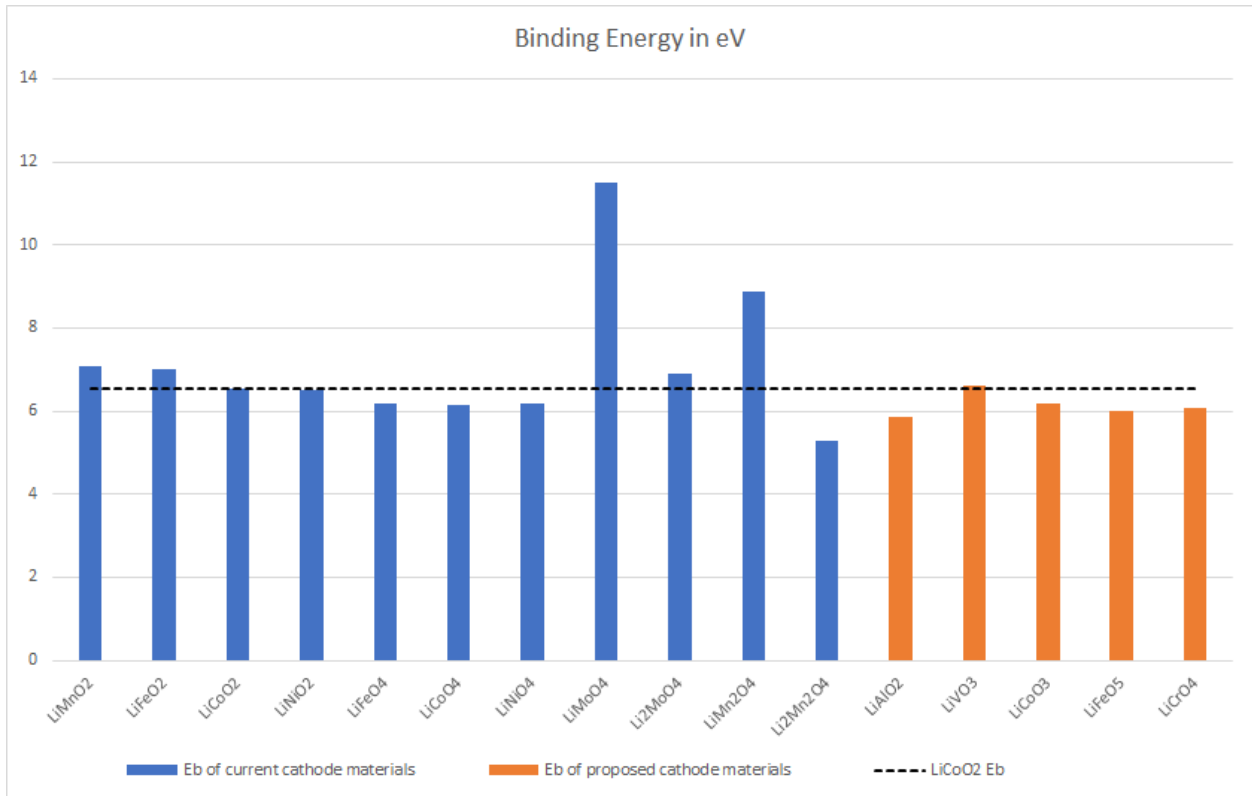


Figure 26 Binding Energy of current and proposed cathode materials

3.3.6 Next Steps

The next step is to analyze the crystalline structure of the new cathode materials investigated here. Additional research should be undertaken to see if the energetics of the crystal to remove the Li^+ cation is commensurate with the trend seen in the results presented in this thesis.

Determining additional properties of the materials, like melting point, and mechanical properties, like flexibility and gravimetric density, would be beneficial for assessing the suitability of the materials for LIBs.

4. Outlook

Increased demand from portable electronics and from the need to store electricity generated from renewable sources has ignited research into LIBs over the last two decades. These rechargeable batteries have achieved a critical balance of weight, size, lifetime, and performance capabilities to make them ubiquitous in modern life. With demand for even greater performance, research will certainly continue in pursuit of the next breakthrough. Portable and high energy batteries are in great demand in today's society, and research and development will continue to push future performance to new levels. There will certainly be incremental advancements in materials, as have been modestly proposed in this thesis, as well as many revolutionary changes in designs and technologies. While the focus of this thesis has been a theoretical look at cathode materials and possible direction for future incremental research, the state of the technology is poised for significant progress along several paths, a few of which are discussed briefly below.

4.1 Future of Batteries

Many advancements being pursued in rechargeable batteries involve changing components of existing technologies. For instance, liquid organic electrolytes can be upgraded with solid electrolytes, which would also allow for higher performing anode materials. In addition, research is underway to implement batteries for which the underlying active ion is sodium, which certainly offers advantages in safety and cost but at the same time suffers from decreased overall

performance compared to lithium. And, early work on lithium air batteries shows promise for enhanced performance characteristics.

4.1.1 Solid Electrolytes

Many of the safety and durability issues with current LIBs are the result of the liquid organic electrolytes. Overcoming these issues could allow for the use of lithium metal as the anode material, resulting in a 20% increase in energy density.²⁹ Work is also underway to find halogen-free options for solid electrolytes, avoiding the disadvantages of halogens while offering up a bounty of materials options to find the most desirable set of properties.⁵⁰

4.1.2 Sodium Ion

A sodium ion battery works on the same basic principles as a LIB, but with Na^+ as the working ion. The main advantage of sodium over lithium is the vast availability of sodium. It is cheaper and more plentiful, so it is less susceptible to fluctuations in resource supply. The driving factor for the current research is to develop a less expensive battery with side benefits of improved safety and environmental friendliness. While sodium and lithium are chemically similar, sodium has some disadvantages for battery chemistries. A sodium cation has nearly twice the radius of a lithium cation and is less polarizing, so its behavior within the electrodes is less favorable.²² However, research is progressing feverishly to overcome these hurdles because of the advantages to moving toward a safer and more abundant material.

4.1.3 Lithium Air

Lithium air batteries, still in the early stages of research and development, make use of a lithium metal anode, either an aqueous or non-aqueous electrolyte, and a porous cathode. On discharge, Li^+ cations move from the anode to the cathode, where they combine with O_2 from the air.

Lithium air batteries promise high performance, but several obstacles must be overcome, particularly around safety and stability of the electrolyte. Lithium air technology promises radically higher theoretical specific energy, perhaps six times that of current LIBs, to power our future devices.⁵¹

5. Conclusion

The basis of a LIB cathode is lithium, the alkali cation, and a metal oxide, the negative ion. One of our goals for this research is to check the feasibility of replacing the negative ion components of current cathode materials with superhalogens, and, hence, expand the set of possible materials for use in LIB cathodes. Current cathode materials are generally composed of transition metal oxides, and a significant factor for their success is the stability of these TMOs while both lithiated and delithiated. TMOs achieve this stability through their multiple valences. For instance, cobalt forms CoO_2 at valency of 4, but it accommodates the presence of lithium by adopting a valency of 5. To be a viable alternate cathode material, any proposed clusters must demonstrate similar multi-valency.

To achieve the objectives of this thesis, the ground state energies of 14 metal oxide clusters, both neutral and anion complexes, and 16 corresponding lithium-bearing salts were modeled in the Gaussian G03 software using hybrid functional BPW91 and basis set 6-311+G*. Nine of the metal oxides and 11 of the lithium salts are currently in use in LIBs. Their results serve as a benchmark in order to understand the electronic properties of proven materials. Five metal oxides and five corresponding lithium salts are not currently used in LIBs. These metal oxide clusters were chosen because they are superhalogens.

Observations of the resulting ground-state geometries show only small changes between the neutral and anion of each metal oxide for both existing and proposed cathode materials. This

qualitatively suggests only small differences in EA and VDE for each cluster. It also reflects a requirement of the cathode material not to change its structure radically during lithiation and delithiation. Similarly, the addition of the Li^+ cation to the metal oxide anion does not cause profound changes in the geometries of the metal oxides, again confirming a structural stability that makes them suitable for the rigors of multiple charges and discharges.

The electronic properties investigated are electron affinity, vertical detachment energy, and binding energy between the Li^+ cation and the metal oxide anion complex. EAs for the proposed cathode materials were found to be slightly higher than the materials in current use, as was expected with the choice of superhalogens. Higher EAs of the proposed materials may indicate that they will bond more readily with a Li^+ cation, which may give them a performance advantage in a LIB. As suggested in the geometries, calculated VDE values were close to EA values. Where available, known experimental results for both EA and VDE compare favorably with computed results.

Calculated binding energies for the proposed cathode materials were very similar to, though slightly lower than, the materials currently in use. Most values for materials currently in use fell between 6.13 eV and 7.01 eV. The binding energies calculated for the proposed materials were in the range of 5.86 eV and 6.63 eV. As with the findings from EA and VDE, these results suggest that the proposed materials will lithiate and delithiate more readily.

List of References

-
- ¹ Sweet, W.V., R. Horton, R.E. Kopp, A.N. LeGrande, and A. Romanou, 2017: Sea level rise. In: Climate Science Special Report: Fourth National Climate Assessment, Volume I [Wuebbles, D.J., D.W. Fahey, K.A. Hibbard, D.J. Dokken, B.C. Stewart, and T.K. Maycock (eds.)]. U.S. Global Change Research Program, Washington, DC, USA, pp. 333-363, doi: 10.7930/J0VM49F2.
- ² Flechas, J. 2017 January 28. Miami Beach to begin new \$100 million flood prevention project in face of sea level rise. Miami Herald. [updated 2017 March 23, accessed March 2019]. <https://www.miamiherald.com/news/local/community/miami-dade/miami-beach/article129284119.html>
- ³ U.S. Environmental Protection Agency, "Sources of Greenhouse Gas Emissions". [accessed 2019 April]. <https://www.epa.gov/ghgemissions/sources-greenhouse-gas-emissions>
- ⁴ Energy Information Administration (US). Monthly energy review March 2019. Government Printing Office, 2019.
- ⁵ Li, Yong, Jian Song, and Jie Yang. "A review on structure model and energy system design of lithium-ion battery in renewable energy vehicle." Renewable and Sustainable Energy Reviews 37 (2014): 627-633.
- ⁶ Energy Information Administration (US). Monthly energy review March 2019. Government Printing Office, 2019.
- ⁷ Nitta, Naoki, et al. "Li-ion battery materials: present and future." Materials today 18.5 (2015): 252-264.
- ⁸ Bloomberg New Energy Finance. "Sustainable Energy in America: Factbook 2019." Business Council for Sustainable Energy (2019).
- ⁹ Ceder, Gerbrand, et al. "Recharging lithium battery research with first-principles methods." Mrs Bulletin 36.3 (2011): 185-191.
- ¹⁰ Goodenough, John B., and Kyu-Sung Park. "The Li-ion rechargeable battery: a perspective." Journal of the American Chemical Society 135.4 (2013): 1167-1176.

-
- ¹¹ Liu, Chaofeng, Zachary G. Neale, and Guozhong Cao. "Understanding electrochemical potentials of cathode materials in rechargeable batteries." *Materials Today* 19.2 (2016): 109-123.
- ¹² Orendorff, Christopher J., and Daniel H. Doughty. "Lithium ion battery safety." *The Electrochemical Society Interface* 21.2 (2012): 35-35.
- ¹³ Manthiram, Arumugam, Xingwen Yu, and Shaofei Wang. "Lithium battery chemistries enabled by solid-state electrolytes." *Nature Reviews Materials* 2.4 (2017): 16103.
- ¹⁴ Zanini, M., S. Basu, and J. E. Fischer. "Alternate synthesis and reflectivity spectrum of stage 1 lithium—graphite intercalation compound." *Carbon* 16.3 (1978): 211-212.
- ¹⁵ Manthiram, Arumugam. "An outlook on lithium ion battery technology." *ACS central science* 3.10 (2017): 1063-1069.
- ¹⁶ Tarascon, J-M., and Michel Armand. "Issues and challenges facing rechargeable lithium batteries." *Materials for Sustainable Energy: A Collection of Peer-Reviewed Research and Review Articles from Nature Publishing Group*. 2011. 171-179.
- ¹⁷ Goodenough, John B., and Youngsik Kim. "Challenges for rechargeable Li batteries." *Chemistry of materials* 22.3 (2009): 587-603.
- ¹⁸ Winter, Martin. "The solid electrolyte interphase—the most important and the least understood solid electrolyte in rechargeable Li batteries." *Zeitschrift für physikalische Chemie* 223.10-11 (2009): 1395-1406.
- ¹⁹ Google Store, "Google Pixel 2 by the numbers". [accessed 2019 March]. https://store.google.com/us/product/pixel_2_specs?hl=en-US
- ²⁰ Battery Market, "Google G011A-B Pixel 2, 2700mAh Li-Polymer Mobile Phone battery". [accessed 2019 March]. <https://batterymarket.eu/en/google-g011a-b-pixel-2-g011a-2700mah-li-polymer-mobile-phone-battery>
- ²¹ Wang, Aiping, et al. "Review on modeling of the anode solid electrolyte interphase (SEI) for lithium-ion batteries." *npj Computational Materials* 4.1 (2018): 15.
- ²² Nayak, Prasant Kumar, et al. "From Lithium-Ion to Sodium-Ion Batteries: Advantages, Challenges, and Surprises." *Angewandte Chemie International Edition* 57.1 (2018): 102-120.
- ²³ Dillon, Shen J., and Ke Sun. "Microstructural design considerations for Li-ion battery systems." *Current Opinion in Solid State and Materials Science* 16.4 (2012): 153-162.

-
- ²⁴ Aydinol, M. K., et al. "Ab initio study of lithium intercalation in metal oxides and metal dichalcogenides." *Physical Review B* 56.3 (1997): 1354.
- ²⁵ Diouf, Boucar, and Ramchandra Pode. "Potential of lithium-ion batteries in renewable energy." *Renewable Energy* 76 (2015): 375-380.
- ²⁶ Fan, Yanchen, et al. "Modeling and theoretical design of next-generation lithium metal batteries." *Energy Storage Materials* 16 (2019): 169-193.
- ²⁷ Moynihan, Tim. "Don't blame the batteries for every lithium-ion explosion". *Wired*. [2017 March 19; accessed 2019 March]. <https://www.wired.com/2017/03/dont-blame-batteries-every-lithium-ion-explosion/>
- ²⁸ Tarascon, J-M. "Key challenges in future Li-battery research." *Philosophical Transactions of the Royal Society A: Mathematical, Physical and Engineering Sciences* 368.1923 (2010): 3227-3241.
- ²⁹ Ulvestad, Andrew. "A Brief Review of Current Lithium Ion Battery Technology and Potential Solid State Battery Technologies." *arXiv preprint arXiv:1803.04317* (2018).
- ³⁰ Song, J. Y., Y. Y. Wang, and C. Cv Wan. "Review of gel-type polymer electrolytes for lithium-ion batteries." *Journal of power sources* 77.2 (1999): 183-197.
- ³¹ Wu, Cuo, et al. "A review: enhanced anodes of li/Na-ion batteries based on yolk-shell structured nanomaterials." *Nano-micro letters* 10.3 (2018): 40.
- ³² Giri, Santanab, Swayamprabha Behera, and Puru Jena. "Superhalogens as Building Blocks of Halogen-Free Electrolytes in Lithium-Ion Batteries." *Angewandte Chemie International Edition* 53.50 (2014): 13916-13919.
- ³³ Oppenheimer, Julius Robert. "Zur quantentheorie kontinuierlicher spektren." *Zeitschrift für Physik A Hadrons and nuclei* 41.4-5 (1927): 268-293.
- ³⁴ Hartree, Douglas R. "The wave mechanics of an atom with a non-Coulomb central field. Part I. Theory and methods." *Mathematical Proceedings of the Cambridge Philosophical Society*. Vol. 24. No. 1. Cambridge University Press, 1928.
- ³⁵ Fock, V. *Z Physik* (1930) 61: 126. <https://doi.org/10.1007/BF01340294>
- ³⁶ Slater, John C. "The Electronic Structure of Atoms—The Hartree-Fock Method and Correlation." *Reviews of Modern Physics* 35.3 (1963): 484.

-
- ³⁷ Kohn, Walter, and Lu Jeu Sham. "Self-consistent equations including exchange and correlation effects." *Physical review* 140.4A (1965): A1133.
- ³⁸ Perdew, John P. "Unified theory of exchange and correlation beyond the local density approximation." *Electronic structure of solids* 91 11 (1991).
- ³⁹ Tang, Wan Si, et al. "Unparalleled lithium and sodium superionic conduction in solid electrolytes with large monovalent cage-like anions." *Energy & environmental science* 8.12 (2015): 3637-3645.
- ⁴⁰ Mizushima, K., et al. "Li_xCoO₂ (0 < x < 1): A new cathode material for batteries of high energy density." *Materials Research Bulletin* 15.6 (1980): 783-789.
- ⁴¹ Bartlett, Neil. "Xenon Hexafluoroplatinate(v) Xe+[PtF₆]-", *Proceedings of the Chemical Society, London* 6 (1962): 218-220.
- ⁴² Mayer, Martin, et al. "Rational design of an argon-binding superelectrophilic anion." *Proceedings of the National Academy of Sciences* (2019): 201820812.
- ⁴³ Gutsev, G. L., and A. I. Boldyrev. "DVM-X α calculations on the ionization potentials of MX_k+ 1- complex anions and the electron affinities of MX_k+ 1 "superhalogens". *Chemical Physics* 56.3 (1981): 277-283.
- ⁴⁴ Pathak, Biswarup, et al. "Borane Derivatives: A New Class of Super-and Hyperhalogens." *ChemPhysChem* 12.13 (2011): 2423-2428.
- ⁴⁵ Pradhan, Kalpataru, et al. "A systematic study of neutral and charged 3d-metal trioxides and tetraoxides." *The Journal of chemical physics* 134.14 (2011): 144305.
- ⁴⁶ Zhai, Hua-Jin, et al. "Electronic Structure and Chemical Bonding in MO_n- and MO_n Clusters (M= Mo, W; n= 3– 5): A Photoelectron Spectroscopy and ab Initio Study." *Journal of the American Chemical Society* 126.49 (2004): 16134-16141.
- ⁴⁷ Desai, Sunil R., et al. "A study of the structure and bonding of small aluminum oxide clusters by photoelectron spectroscopy: Al_xO_y-(x= 1–2, y= 1–5)." *The Journal of chemical physics* 106.4 (1997): 1309-1317.
- ⁴⁸ Gutsev, G. L., et al. "Electronic structure of chromium oxides, CrO_n- and CrO_n (n= 1–5) from photoelectron spectroscopy and density functional theory calculations." *The Journal of Chemical Physics* 115.17 (2001): 7935-7944.

⁴⁹ Vyboishchikov, Sergei F., and Joachim Sauer. "Gas-phase vanadium oxide anions: Structure and detachment energies from density functional calculations." *The Journal of Physical Chemistry A* 104.46 (2000): 10913-10922.

⁵⁰ Fang, Hong, et al. "Superhalogen-based lithium superionic conductors." *Journal of Materials Chemistry A* 5.26 (2017): 13373-13381.

⁵¹ Choi, Jang Wook, and Doron Aurbach. "Promise and reality of post-lithium-ion batteries with high energy densities." *Nature Reviews Materials* 1.4 (2016): 16013.